

Reproduced by
**NATIONAL TECHNICAL
INFORMATION SERVICE**
Springfield, Va. 22151

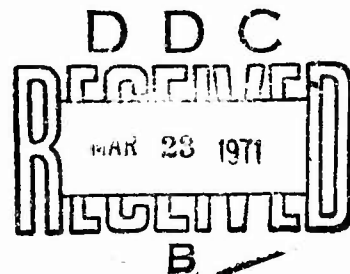


CONTRACT REPORT S-70-7

CRACKING OF EARTH AND ROCKFILL DAMS TENSION ZONES IN EMBANKMENTS CAUSED BY CONDUITS AND CUTOFF WALLS

by

A. Casagrande, S. W. Covarrubias



July 1970

Sponsored by Office, Chief of Engineers, U. S. Army

Conducted for U. S. Army Engineer Waterways Experiment Station, Vicksburg, Mississippi

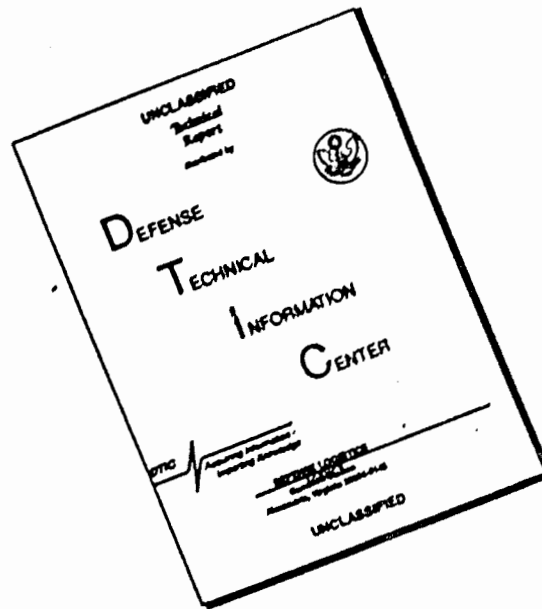
Under Contract No. DACW 39-69-C-0029

By Harvard University, Cambridge, Massachusetts

ARMY-MRC VICKSBURG, MISS

This document has been approved for public release and sale; its distribution is unlimited

DISCLAIMER NOTICE



THIS DOCUMENT IS BEST QUALITY AVAILABLE. THE COPY FURNISHED TO DTIC CONTAINED A SIGNIFICANT NUMBER OF PAGES WHICH DO NOT REPRODUCE LEGIBLY.

PREFACE

The work described in this report was performed under Contract No. DACW 39-60-C-0029, "Cracking of Earth Dams," between the U. S. Army Engineer Waterways Experiment Station (WES) and Harvard University. The contract was sponsored by the Office, Chief of Engineers, under Engineering Studies Item ES-544, "Cracking of Earth Dams."

The general objective of this research, which began in 1968, was to investigate by the finite element method the factors that influence cracking in earth dams. Work on this project was conducted under the supervision of Arthur Casagrande, Professor of Soil Mechanics and Foundation Engineering. The project was administered by the President and Fellows of Harvard University. The report was prepared by Arthur Casagrande and S. W. Covarrubias.

The contract was monitored at WES by Mr. J. B. Palmerton, Rock Mechanics Section, Soil and Rock Mechanics Branch, Soils Division. Mr. J. P. Sale was Chief of the Soils Division during the preparation and publication of this report. Contracting Officers were, successively, COL Levi A. Brown, CE, and COL Ernest D. Peixotto, CE, Directors of WES. Technical Director of WES during this time was Mr. F. R. Brown.

FOREWORD

The investigations reported herein were performed in partial fulfillment of Contract No. DACW 39-69-C-0029 between the U. S. Army Engineer Waterways Experiment Station and Harvard University, dated 26 March 1969, and of the modification of this Contract effective 15 August 1969. The general purpose and scope of this Contract was stated as follows:

" . . . to investigate factors influencing the development of cracks in earth dams using the finite element method to determine stress and strain distribution in earth dams for a variety of typical boundary conditions (in particular, various shapes of abutments), and of stress-strain properties of the materials in the dam and its foundations. Dams which have cracked will be analyzed to establish empirical correlations between analytical results and actual performance."

This scope was later enlarged to include the following studies:

- (1) Investigation of factors affecting the development of tension zones around conduits in earth embankments.
- (2) Investigation of tension zones caused by rigid cutoff wall beneath an earth dam.
- (3) Investigation of additional case records to compare observed tensile strains along the crest with the results of analyses by means of the finite element method.

The original Contract was fulfilled by the doctoral thesis of Sergio Covarrubias entitled "Cracking of Earth and Rockfill Dams; A Theoretical Investigation by Means of the Finite Element Method," published as WES Contract Report S-69-5, April 1969. Items (1) and (2) above are fulfilled by the present report and item (3) will be fulfilled by a forthcoming report.

Preceding page blank

TABLE OF CONTENTS

| | Page |
|---|------|
| FOREWORD | 3 |
| TABLE OF CONTENTS | 5 |
| LIST OF TABLES | 6 |
| LIST OF FIGURES | 7 |
| LIST OF NOTATIONS | 9 |
| SYNOPSIS | 10 |
| CHAPTER 1. INTRODUCTION | |
| 1.1 PURPOSE AND SCOPE | 11 |
| 1.2 BASIC APPROACH | 11 |
| 1.3 METHOD OF ANALYSIS | 12 |
| CHAPTER 2. TENSION ZONES IN AN EMBANKMENT ON A RIGID FOUNDATION CAUSED BY A RIGID CONDUIT | |
| 2.1 GENERAL | 13 |
| 2.2 CONDUIT IN HOMOGENEOUS FILL | 13 |
| 2.3 USE OF A COMPRESSIBLE ZONE TO CONTROL LOADING ON CONDUIT | 15 |
| 2.4 DISCUSSION OF RESULTS | 17 |
| CHAPTER 3. TENSION ZONES IN AN EMBANKMENT AND ITS FOUNDATION CAUSED BY A RIGIDLY SUPPORTED CUTOFF WALL | |
| 3.1 GENERAL | 19 |
| 3.2 CASE A. THICK CUTOFF WALL WITH ROUGH SIDES | 20 |
| 3.3 CASE B. THICK CUTOFF WALL WITH SLIPPERY SIDES | 22 |
| 3.4 CASE C. COMPRESSIBLE ZONE ON TOP OF A THICK CUTOFF WALL WITH ROUGH SIDES | 23 |
| 3.5 CASE D. THIN CUTOFF WALL WITH ROUGH SIDES | 24 |
| 3.6 DISCUSSION OF RESULTS | 26 |
| TABLES | 28 |
| FIGURES | 29 |

Preceding page blank

LIST OF TABLES**Table No**

- | | |
|---|--|
| 1 | Results of Finite Element Analysis of Embankment Surrounding Rigid Conduits |
| 2 | Results of Finite Element Analysis of Embankment with Rigidly Supported Cutoff Wall |




LIST OF FIGURES

Fig. No.

- | | |
|------|--|
| 1 | Geometry of conduits studied |
| 2(a) | Principal stresses in fill surrounding semi-elliptical conduit |
| 2(b) | Normal stresses acting on the sides of semi-elliptical conduit |
| 3(a) | Principal stresses in fill surrounding square conduit with H/D ratio of 5 |
| 3(b) | Normal stresses acting on the sides of square conduit with H/D ratio of 5 |
| 4(a) | Principal stresses in fill surrounding square conduit with H/D ratio of 10 |
| 4(b) | Normal stresses acting on the sides of square conduit with H/D ratio of 10 |
| 5(a) | Principal stresses in fill surrounding square conduit; Compressibility ratio of 1/2 |
| 5(b) | Normal stresses acting on the sides of square conduit; Compressibility ratio of 1/2 |
| 6(a) | Principal stresses in fill surrounding square conduit; Compressibility ratio of 1/5 |
| 6(b) | Normal stresses acting on the sides of square conduit; Compressibility ratio of 1/5 |
| 7(a) | Principal stresses in fill surrounding square conduit; Compressibility ratio of 1/10 |
| 7(b) | Normal stresses acting on the sides of square conduit; Compressibility ratio of 1/10 |

- 8 Loading ratio for square conduit as function of compressibility ratio
- 9(a) Geometry of dam used in Cases A, B and C
- 9(b) Geometry of dam used in Case D
- 10(a) Displacements in dam and foundation, Case A
- 10(b) Principal stresses in dam and foundation, Case A
- 10(c) Stresses acting on one side of the wall, Case A
- 11(a) Displacements in dam and foundation, Case B
- 11(b) Principal stresses in dam and foundation, Case B
- 12(a) Displacements in dam and foundation, Case C
- 12(b) Principal stresses in dam and foundation, Case C
- 12(c) Stresses acting on one side of the wall, Case C
- 13(a) Displacements in dam and foundation, Case D
- 13(b) Principal stresses in dam and foundation, Case D
- 13(c) Stresses acting on one side of the wall, Case D

LIST OF NOTATIONS

| | |
|---|---|
| D | height and width of conduit, m |
| E_c | modulus of elasticity of a highly compressible zone above the conduit, kg/sq cm |
| E_f | modulus of elasticity of fill, kg/sq cm |
| F | vertical force per unit of length along foundation of cutoff wall caused by negative skin friction, kg/cm |
| H | height of embankment, m |
| K_o | coefficient of earth pressure at rest |
| p_h | normal stress at mid-height of conduit, kg/sq cm |
| p_v | normal stress at center of crown of conduit, kg/sq cm |
| s | potential maximum shearing resistance along sides of cutoff wall, kg/sq cm |
| γ | unit weight, kg/cu m |
| ν | Poisson's ratio |
| σ_v | vertical stress on top surface of cutoff wall, kg/sq cm |
| τ | shear stress along sides of wall, kg/sq cm |
|  | rigid fixed boundary |
|  | slippery boundary |
|  | axis of symmetry |

SYNOPSIS

The purpose of this study was to investigate by means of the finite element method (1) the effect of rigid conduits and cutoff walls on the stress distribution and on the development of tension zones in embankments and their foundations, and (2) the distribution of stresses acting on the sides of conduits and cutoff walls.

All materials were assumed to be linearly elastic with equal properties in tension and in compression. The only load considered was the weight of the embankment and it was assumed to be applied in a single lift.

Detailed investigation by means of the finite element method included six cases of conduits and four cases of cutoff walls. In the case of conduits, it was demonstrated that tension zones occur adjacent to conduits with sharp edges, and that the presence of a zone of more compressible material above the roof effectively improves the loading conditions on the conduit. In the case of cutoff walls beneath embankments, it was shown that tension zones develop in the upper part of the embankment and adjacent to the top of the wall. While the presence of a zone of more compressible material on top of the wall reduces the load on the upper surface of the wall, it somewhat increases the friction forces along the sides of the wall.

CHAPTER 1

INTRODUCTION

1.1 PURPOSE AND SCOPE

The purpose of this study was to investigate by means of the finite element method (1) the effect of rigid conduits and cutoff walls on the stress distribution and on the development of tension zones in embankments and their foundations, and (2) the distribution of stresses acting on the sides of conduits and cutoff walls.

Conduits — All conduits were assumed to be rigid and to be supported directly on an incompressible base which also forms the foundation of the embankment. The following variables were investigated: (1) shape of conduit; (2) thickness of overlying embankment; and (3) effect of a more compressible zone located immediately over the conduit.

Cutoff Walls — Four cases were analyzed: (1) a thick cutoff wall with rough sides, i.e. assuming no relative displacements between the wall and the adjacent soil; (2) a thick slippery cutoff wall, i.e. assuming no shear stresses on the sides of the wall; (3) a thick rough cutoff wall with a compressible zone on top of the wall; and (4) a thin cutoff wall with rough sides. Particular attention was also paid to the distribution of normal and shear stresses along the sides of the wall in an effort to determine the vertical load on the wall produced by negative skin friction.

1.2 BASIC APPROACH

The studies under Contract No. DACW 39-69-C-0029 are based on the senior author's concept that for the purpose of investigating tension zones and cracking in embankments it is of advantage to assume that all materials are perfectly elastic and that although such simplification of the stress-strain properties of the materials exaggerates the magnitude of the tensile stresses, it does not significantly

change the geometry of the tension zones and the locations of the maximum tensile stresses as compared to those that develop in an actual embankment. This hypothesis was thoroughly investigated by the junior author in his doctoral thesis (Covarrubias, 1969)* where he compared observational data of several dams with the results of the finite element analysis of these dams and found good agreement, thus demonstrating the usefulness of this approach.

1.3 METHOD OF ANALYSIS

The method of analysis and the computer program are the same as described by Covarrubias (1969,* Chapter 3 and Appendix).

The finite element method as used in this investigation yields values of stresses at the centroids of the elements. Linear extrapolation was used to evaluate the stresses at the boundaries of the sections analyzed.

* Covarrubias, S. W. (1969), "Cracking of Earth and Rockfill Dams," Harvard Soil Mechanics Series No. 82, Harvard University, Cambridge, Mass.

CHAPTER 2

TENSION ZONES IN AN EMBANKMENT ON A RIGID FOUNDATION CAUSED BY A RIGID CONDUIT

2.1 GENERAL

The influence of the following variables on the development of tension zones and on the stresses acting on the conduit was investigated: (1) shape of conduit, (2) thickness of overlying fill, and (3) effect of a more compressible zone located immediately over the conduit. The conduits were assumed to be 5 x 5 m, either square or semi-elliptical, and resting directly on the incompressible foundation. By exaggerating conventional shapes of conduits, a better insight into the effect of the geometry of the conduit was obtained.

2.2 CONDUIT IN HOMOGENEOUS FILL

Three cases with homogeneous fill, illustrated in Fig. 1, were investigated. The fill is assumed to have the following properties:

| | | |
|-----------------|---|---------------|
| Unit weight | = | 1 900 kg/cu m |
| Young's modulus | = | 200 kg/sq cm |
| Poisson's ratio | = | 0.35 |

For the sake of analysis, vertical, rigid-slippery boundaries are assumed 20 m from the centerline of the conduit.

Case A — Semi-elliptical Conduit with Ratio of Height of Embankment to Width of Conduit $H/D = 5$

Fig. 2(a) shows (1) the pertinent dimensions and (2) the principal stresses in the embankment. With the height of the embankment $H = 25$ m and the width of the

conduit $D = 5$ m, the ratio is $H/D = 5$. As can be seen, no tensile stresses are induced in the fill adjacent to this conduit, but there is a zone of tensile stresses along the surface of the fill. This zone extends about 10 meters on both sides of the centerline of the conduit. Its maximum depth is 1.2 meters and the maximum tensile stress is only 0.1 kg/sq cm. Both occur along the centerline of the conduit. By comparison with the investigations by Covarrubias (1969), it is concluded that tensile stresses of this order of magnitude normally will not produce tensile cracks.

In Fig. 2(b) are plotted the normal stresses on the surface of the conduit, which have values of $p_v = 6.6$ kg/sq cm at the center of the crown and $p_h = 2.7$ kg/sq cm at mid-height of the conduit. These values define the loading ratio $p_v/p_h = 2.4$.

Case B — Square Conduit with $H/D = 5$

Fig. 3(a) shows (1) the pertinent dimensions and (2) the principal stresses in the embankment. Adjacent to the upper portion of the sides of the conduit there are small tension zones with a maximum tensile stress of about 0.9 kg/sq cm along the upper edges. The tension zone along the surface of the fill is similar to that in the preceding case, with a maximum tensile stress at the surface of about 0.2 kg/sq cm along the centerline of the conduit. Depending chiefly on the stress-strain characteristics of the fill, the tension zone adjacent to the side walls of the conduit might induce "piping" along the conduit.

In Fig. 3(b) are plotted the normal stresses on the surface of the conduit. On the roof the normal stress ranges from about 5 kg/sq cm along the centerline to about 8 kg/sq cm along the edges, and along the middle of the sides it is about 2 kg/sq cm. The loading ratio $p_v/p_h = 5/2 = 2.5$ is slightly greater than for the elliptical conduit, Case A.

Case C — Square Conduit with $H/D = 10$

To investigate the effect of a much larger H/D ratio on the tension zone

adjacent to the square conduit without having to resort to preparation of a new set of data cards for the computer program, a surcharge of 4.75 kg/sq cm, which is equivalent to an additional 25-meter height of fill, was superposed on Case B. For practical purposes this procedure yields the same stresses in the immediate vicinity of the conduit as would be obtained for a 50-meter high fill to start with.

Fig. 4(a) shows the distribution of principal stresses in the vicinity of the conduit. It can be seen that the tension zones adjacent to the upper portion of the sides are smaller than for Case B, but the maximum tensile stress of 1.8 kg/sq cm is twice as great as for Case B. Although the much greater maximum tensile stress suggests a more dangerous condition, the greater height of fill would also produce a greater tendency for the crack to close by creep deformation in the fill.

In Fig. 4(b) are plotted the normal stresses on the surface of the conduit. On the roof, the normal stress ranges from about 11 kg/sq cm along the center-line to about 15 kg/sq cm along the edges, and along the middle of the sides it is about 4.2 kg/sq cm. The loading ratio $p_v/p_h = 2.5$ is the same as for the preceding Case B.

2.3 USE OF A COMPRESSIBLE ZONE TO CONTROL LOADING ON CONDUIT

The most effective method for improving the stress distribution around a conduit, i.e. to achieve a loading ratio p_v/p_h close to one, is the addition of a more compressible zone on top of the conduit. Three cases have been investigated in which the dimensions of the compressible zone are assumed to be identical with the dimensions of the 5 x 5-meter square conduit, and using compressibility ratios E_c/E_f , i.e. ratios of the modulus of elasticity E_c of the more compressible zone to the modulus of elasticity E_f of the fill material, of 0.5, 0.2 and 0.1. The unit weight and Poisson's ratio of the compressible zone are assumed equal to those of the fill material.

Case D — Compressibility Ratio $E_c/E_f = 0.5$

Fig. 5(a) shows (1) the pertinent dimensions and (2) the principal stresses in the fill. Adjacent to the upper portions of the sides of the conduit there are small tension zones with a maximum tensile stress of about 1.2 kg/sq cm along the upper edges. The tension zone along the crest of the fill is similar to the case of the homogeneous fill in Fig 3(a).

As can be seen in Fig. 5(b) the vertical stresses on the roof of the conduit increase from a value of 3.8 kg/sq cm along the centerline to about 5.0 kg/sq cm along the edges. The maximum horizontal stress along the sides, of about 2.1 kg/sq cm occurs at about mid-height on the conduit. The loading ratio, $p_v/p_h = 1.8$, is about 70% of the corresponding value in Case B without the compressible zone.

Case E — Compressibility Ratio $E_c/E_f = 0.2$

For the same dimensions as in Fig. 5(a), but for a compressibility ratio of 0.2, the distribution of the principal stresses and of the tension zones along the crest of the fill and along the sides of the conduit are shown in Fig. 6(a). Now there is no tension zone along the middle of the crest, but there are tension zones along both ends of the crest, with maximum tensile stresses of about 0.06 kg/sq cm at the ends. The tension zones along the sides of the conduit have a maximum tensile stress of about 1.3 kg/sq cm along the upper edges.

Fig. 6(b) shows the distribution of normal stresses on the surface of the conduit. On the roof the normal stresses range from 2.3 kg/sq cm along the centerline to about 2.9 kg/sq cm along the edges. The maximum horizontal stress along the sides is about 2.3 kg/sq cm and occurs at about mid-height on the conduit. Therefore, one achieves in this case the ideal loading ratio $p_v/p_h = 1.0$.

Case F — Compressibility Ratio $E_c/E_f = 0.1$

For the same dimensions as in Fig. 5(a), but for a compressibility ratio of

0.1, the distribution of the principal stresses and of the tension zones along the crest of the fill and along the sides of the conduit are shown in Fig. 7(a). Again there are two tension zones along both ends of the crest, with a maximum tensile stress of about 0.1 kg/sq cm at the ends. The maximum tensile stress along the sides of the conduit is about 1.3 kg/sq cm and is again located along the upper edges.

Fig 7(b) shows the distribution of normal stresses on the surface of the conduit. On the roof the normal stresses range from 1.8 kg/sq cm along the centerline to 2.0 kg/sq cm along the edges, and the maximum horizontal stress along the sides of about 2.5 kg/sq cm occurs about mid-height of the conduit. Thus, the loading ratio is $p_v/p_h = 0.7$, i.e. less than unity.

2.4 DISCUSSION OF RESULTS

Table 1 is a summary of the most important results in this chapter.

Tension Zones Along Crest of Dam — For the investigated H/D ratios of 5 and 10 the maximum induced tensile stresses are so small that they would not produce tension cracks.

Tension Zones Adjacent to Conduit — For square conduits small tension zones occur in the fill adjacent to the upper portions of the sides of the conduits. The tensile stresses that develop may cause formation of tension cracks in the fill. Such cracks, combined with the possibility that the soil will pull away from the side walls near the upper edges, may induce "piping" along the conduit walls.

With increasing ratio H/D the tension zones adjacent to square conduits decrease slightly in size, but the maximum tensile stress increases substantially.

For the semi-elliptical conduit the analysis yielded no tension zones adjacent

to the conduit. This result suggests that sharp edges should be avoided on the outside of conduits.

Effect of Highly Compressible Zone over a Conduit — The presence of a highly compressible zone over the roof of a conduit effectively reduces the magnitude of the vertical stresses on the roof and slightly increases the horizontal stresses on the sides of the conduit. By appropriate choice of the height of the compressible zone and of the compressibility ratio a desired loading ratio can be achieved. For the geometry illustrated in Fig. 1, the results plotted in Fig. 8 show that for a compressibility ratio E_c/E_f of about 0.2, one achieves a loading ratio $p_v/p_h = 1.0$, i.e. a hydrostatic loading condition.

CHAPTER 3

TENSION ZONES IN AN EMBANKMENT AND ITS FOUNDATION CAUSED BY A RIGIDLY SUPPORTED CUTOFF WALL

3.1 GENERAL

In this chapter are presented the results of investigations of the following four cases:

Case A. Stress distribution in an embankment and in its compressible foundation, with a thick rigid-rough cutoff wall through the foundation, i.e. with zero relative displacements between the wall and the adjacent soil.

Case B. Same as Case A, except that the surfaces of the cutoff wall are assumed to be "slippery", i.e. no friction forces are transmitted between the wall and the soil.

Case C. Same as Case A, except that a zone of highly compressible material is placed immediately above the top of the cutoff wall.

Case D. Same as Case A, except that the rigid-rough cutoff wall is assumed to have zero thickness.

The distribution of stresses acting on the sides of the cutoff wall is studied in an effort to determine the order of magnitude of the vertical stresses in the wall which are produced by the weight of the embankment.

For Cases A, B and C, the geometry of the embankment is shown in Fig. 9(a). It is 100 m high, with side slopes of 1 (vertical) on 3 (horizontal), and rests on a 100-m-thick foundation stratum which has the same compressibility as the embankment and which in turn is underlain by a horizontal rigid-rough surface. Along the centerline a 10-m-wide rigid cutoff wall extends through the compressible foundation stratum, i.e. from the base of the dam down to the rigid underlying rock.

For Case D, the geometry of the embankment is shown in Fig. 9(b). It has the same height, side slopes and foundation stratum as in cases A, B and C, but the

rigid-rough wall is assumed to have a zero thickness.

For convenience of analysis, in all cases vertical "slippery" boundaries are assumed on both sides of the embankment at distances of 500 m from the centerline. In addition, it is assumed that the compressible foundation deforms only under the weight of the embankment and not under its own weight, which is equivalent to assume zero unit weight for the foundation soil. The assumed material properties are listed below:

| Zone | Young's Modulus kg/sq cm | Poisson's ratio | Unit weight kg/cu m |
|------------|--------------------------------|--------------------|---------------------------|
| Embankment | 200 | 0.35 | 1 900 |
| Foundation | 200 | 0.35 | 0 |

3.2 CASE A. THICK CUTOFF WALL WITH ROUGH SIDES

In Case A the wall is assumed to be "rough," i.e. no relative movements can develop between the wall and the adjacent soil.

Fig. 10(a) shows the displacements of points within the embankment and within the foundation. The maximum settlement of 5.72 m occurs at the centerline of the crest. The maximum settlement of the foundation surface (base of embankment) of 3.83 m occurs about 90 m from the centerline.

Fig. 10(b) shows the distribution of the principal stresses, and the locations of the tension zones in the embankment and in the foundation. The tension zone in the top of the embankment is roughly triangular and extends from the crest to about 72 m down the slopes and to a depth of about 50 m beneath the crest. The maximum tensile stress of about 2.4 kg/sq cm occurs on the slope at a distance of approximately 20 m from the crest.

The tension zones in the foundation stratum occur adjacent to the upper part of the cutoff wall. They extend over a depth of 40 m, with a maximum width

of 13 m. The maximum tensile stress of about 13 kg/sq cm occurs adjacent to the top edges of the cutoff wall.

The vertical stresses σ_v on the top surface of the wall are about 44 kg/sq cm, which is about 2.3 times larger than the vertical stress under a 100-m-high column of embankment material.

In Fig. 10(c) are shown (1) the distribution of effective horizontal stresses acting on the sides of the wall, (2) the potential maximum shearing resistance along the wall, and (3) the computed shear stresses along the wall produced by the weight of the embankment. The stresses (1) are the sum of: (a) the in situ effective horizontal stresses in the foundation stratum (computed for a submerged specific gravity of unity and a coefficient of earth pressure at rest $K_0 = 0.5$); and (b) the horizontal stresses produced by the weight of the embankment. The stresses (2) are computed assuming a coefficient of wall friction of 0.5. The shear stresses (3) are computed by means of the finite element method.

The effective horizontal stresses acting on the sides of the wall are compressive over almost the entire length of the wall, but near the top of the wall, they decrease abruptly and rapidly and become tensile stresses over the upper 5 m of the wall. The potential maximum shearing resistance is sensibly uniform over most of the height of the cutoff wall, with a maximum value of about 4.3 kg/sq cm approximately at mid-height. The shear stresses produced by the weight of the embankment exceed 21 kg/sq cm at the top of the wall, and they decrease rapidly with depth. At a depth of 45 m below the base of the embankment both the shear stress and the potential maximum shearing resistance are equal, and below that depth the shear stresses are smaller than the potential maximum shearing resistance.

Assuming that the shear stresses which are transferred from the surrounding soil mass to the wall are equal to the shear stresses produced on the wall by the weight of the embankment, but not greater than the potential maximum shearing resistance, and integrating those stresses over the length of the wall, the total force transmitted

to bedrock through the base of the wall due to negative skin friction over one side of the wall is 23,760 kg/cm of wall length. Assuming a 28-day compressive strength of the concrete of 200 kg/sq cm, one would need a 2.4-m-thick wall to avoid crushing of the lowest portion of the wall by the load produced by negative skin friction which would develop in the course of years.

3.3 CASE B. THICK CUTOFF WALL WITH SLIPPERY SIDES

Case B is similar to Case A, except that the sides of the cutoff wall are assumed to be slippery. Therefore, the shear stresses along the wall are zero and the soil adjacent to the wall can displace vertically.

Fig. 11(a) shows the displacements of points within the embankment and within the foundation. The maximum settlement of 6.03 m occurs at the centerline of the crest. The maximum settlement of the foundation surface (base of embankment) of 3.99 m occurs about 90 m from the centerline. Both of the movements are slightly greater than for Case A because of the freedom of movement at the wall.

Fig. 11(b) shows the distribution of the principal stresses and the locations of the tension zones in the embankment and in the foundation. The tension zone in the top of the embankment is roughly triangular and extends from the crest to about 70 m down the slopes and to a depth of about 52 m beneath the crest. The maximum tensile stress of about 2 kg/sq cm occurs on the slopes at a distance of about 20 m from the crest.

The tension zones in the foundation stratum appear adjacent to the upper part of the cutoff wall, extending over a depth of 19 m, with a maximum width of 15 m. The maximum tensile stress of about 30 kg/sq cm occurs adjacent to the top edges of the cutoff wall.

The vertical stresses on the top surface of the wall are about 50 kg/sq cm,

i.e. approximately 2.6 times larger than the stress under a 100-m-high column of embankment material. In this case, since the wall has been assumed to be slippery, the wall is not loaded by negative skin friction.

3.4 CASE C. COMPRESSIBLE ZONE ON TOP OF A THICK CUTOFF WALL WITH ROUGH SIDES

Case C is similar to Case A, except for the assumption of a compressible zone on top of the cutoff wall with Young's modulus 10 times smaller than the modulus in the embankment proper, and a 10 x 10-m cross section.

Fig. 12(a) shows the displacements of points within the embankment and within the foundation. The maximum settlement of 6.13 m occurs at the centerline of the crest. The maximum settlement of the foundation surface (base of embankment) of 3.90 m occurs about 90 m from the centerline.

Fig. 12(b) shows the distribution of principal stresses and the locations of the tension zones in the embankment and in the foundation. The tension zone in the top of the embankment is almost triangular and extends from the crest about 70 m along the slopes and to a depth of about 45 m beneath the crest. The maximum tensile stress of about 1.5 kg/sq cm occurs on the slopes at a distance of approximately 20 m from the crest.

The tension zones in the foundation occur adjacent to the upper half of the cutoff wall and have a maximum width of 13 m. The maximum tensile stress of about 16 kg/sq cm occurs adjacent to the upper edges of the cutoff wall.

The vertical stresses on the top surface of the wall are about 8.5 kg/sq cm, which is only about one-half of the vertical stress under a 100-m-high column of embankment material.

In Fig. 12(c) are shown: (1) the distribution of effective stresses acting on the sides of the wall, with the same assumptions of specific gravity and K_0 as in Case A, (2) the potential maximum shearing resistance along the wall using the same value of the coefficient of wall friction as in Case A, and (3) the shear stresses along the wall caused by the weight of the embankment.

The effective horizontal stresses, which are compressible over almost the entire height of the wall, decrease abruptly near the top and become tensile stresses over the top 7 m of the wall. The potential maximum shearing resistance has two maxima: (1) about 5.3 kg/sq cm approximately 15 m below the top of the wall, and (2) about 4.5 kg/sq cm approximately 70 m below the top of the wall. At the top of the wall, the shear stresses caused by the weight of the embankment exceed 28 kg/sq cm and decrease rapidly with depth. At a depth of 48 m below the top of the wall, both the shear stress and the shearing resistance are equal. Below that depth the shear stresses are smaller than the potential maximum shearing resistance. The total force transmitted to the base of the wall by negative skin friction is 26,520 kg/cm for each side of the wall.

As compared to Case A, for Case C (1) the computed settlements are larger, (2) the tension zone in the embankment is smaller, (3) the maximum tensile stress in the embankment is substantially smaller, (4) the tension zone in the foundation stratum is slightly deeper, and (5) the maximum tensile stress in the foundation is greater.

3.5 CASE D. THIN CUTOFF WALL WITH ROUGH SIDES

Case D is similar to Case A, except that the cutoff wall which extends through the foundation is assumed to have zero thickness.

Fig. 13(a) shows the displacements of points within the embankment and within the foundation. The maximum settlement of 6.37 m occurs at the centerline of the

crest. The maximum settlement of the foundation surface (base of embankment) of 3.98 m occurs about 90 m from the centerline.

Fig. 13(b) shows the distribution of principal stresses and the locations of the tension zones in the embankment and in the foundation. The tension zone in the top of the embankment is roughly triangular and extends from the crest about 60 m along the slopes and to a depth of about 50 m beneath the crest. The maximum tensile stress of about 1.5 kg/sq cm occurs on the slopes approximately 20 m from the crest.

The tension zones in the foundation extend adjacent to the upper 44 m of the cutoff wall and have a maximum width of 13 m. The maximum tensile stress of about 15 kg/sq cm occurs adjacent to the upper edges of the cutoff wall.

In Fig. 13(c) are shown: (1) the distribution of effective stresses acting on the sides of the wall, with the same assumptions of specific gravity and K_0 as in Case A, (2) the potential maximum shearing resistance along the wall with the same value of the coefficient of wall friction as in Case A, and (3) the shear stresses along the wall caused by the weight of the embankment.

The effective horizontal stresses acting on the sides of the wall, which are compressive over almost the entire length of the wall, decrease abruptly near the top and become tensile stresses over the top 3 m of the wall. The potential maximum shearing resistance is sensibly uniform over almost the entire height of the cutoff wall, with a maximum value of about 4.5 kg/sq cm approximately 65 m below the top of the wall. The shear stresses caused by the weight of the embankment exceed 21 kg/sq cm at the top of the wall, and they decrease rapidly with depth. At a depth of 45 m below the top of the wall, both the shear stress and the shearing resistance are equal, and below that depth the shear stresses are smaller than the

potential maximum shearing resistance. With the same assumptions as stated in Case A, the total force transmitted to the foundation through the base of the wall, caused by negative skin friction, is 25,400 kg/cm for each side of the wall.

3.6 DISCUSSION OF RESULTS

Table 2 is a summary of the important numerical results in this chapter. For the geometry studied, which is shown in Figs. 9(a) and 9(b), the most important conclusions are:

- (1) The presence of a rigid cutoff wall induces substantial tension zones in the embankment and in its foundation.
- (2) Large forces can be transmitted by negative skin friction from the soil to the cutoff wall which may exceed the strength of the wall in its lower portion.

Tension Zones in the Embankment — The tension zone produced in the embankment by a rigid cutoff wall is always located at the top of the embankment, with the maximum tensile stresses along the slopes.

The largest tensile stress in the embankment occurs for the case of a thick cutoff wall with rigid-rough sides, Case A, while the smallest tensile stresses occur for Case C, a thick cutoff wall with rigid-rough sides and with a highly compressible zone on top of the wall, and for Case D, a thin cutoff wall with rigid-rough sides. The computed values of the maximum tensile stress ranged from 1.5 kg/sq cm (Cases C and D) to 2.4 kg/sq cm (Case A), which are relatively small as compared with those computed by Covarrubias (1969) in actual dams that have cracked.

Tension Zones in the Foundation Stratum — The tension zones in the

foundation stratum are located adjacent to the upper part of the cutoff wall, with the maximum tensile stress occurring along the top edges of the wall. The magnitude of the maximum tensile stress is greatest for the case of a thick cutoff wall with rigid-slippery sides, Case B. There are no large differences among the other cases. The maximum tensile stresses range from 13 to 30 kg/sq cm, values which no soil can withstand. However, at such depths the plasticity and time-dependent properties of soils may play an important role in effecting substantial redistribution of stresses.

Vertical Stresses on the Top of the Wall — The vertical stresses acting on the top surface of the wall are effectively reduced by the presence of a zone of more compressible material over the top of the wall. When the more compressible zone is ten times more compressible than the surrounding fill, Case C, the vertical stress is only 25% of the corresponding stress in a homogeneous embankment, Case A, or 0.45 times the weight of a column of soil equal to the height of the embankment.

Stresses and Friction on the Side of the Wall — The effective horizontal stresses that act against the wall are tensile stresses over a small region along the upper part of the wall and they change rapidly with depth to become compressive at 3 to 8-m depth. In homogeneous embankments (Cases A, B and D) the distribution of the effective horizontal stresses is rather uniform over most of the wall, while for Case C it shows two maxima approximately at the third points of the wall.

In all cases, the computed shear stresses on the side of the wall caused by the weight of the embankment, are extremely large along the upper part of the cutoff wall and decrease rapidly with depth.

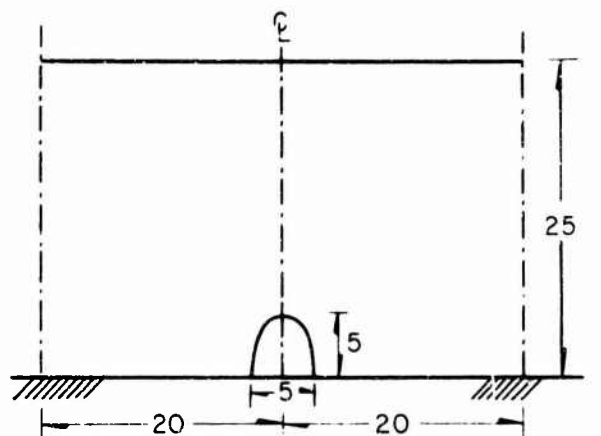
The negative skin friction is slightly larger for the case in which a highly compressible zone is assumed on top of the wall, Case C. However, the presence of the compressible zone results in a small downward force on top of the wall. The difference in negative skin friction between Case C and the other cases is not substantial.

TABLE 1
RESULTS OF FINITE ELEMENT ANALYSIS OF EMBANKMENT
SURROUNDING RIGID CONDUITS

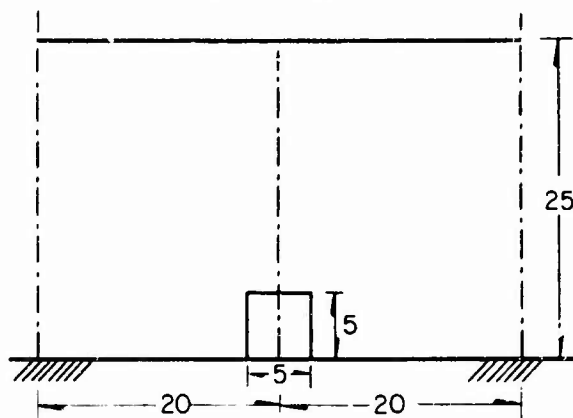
| Case | H/D | Compress- ibility ratio E_c/E_f | Maximum tensile stress in the crest | Maximum tensile stress adjacent to conduit | Loading ratio p_v/p_h |
|------|-----|--|---|--|-------------------------------|
| | | | kg/sq cm | kg/sq cm | |
| A | 5 | 1 | 0.1 | — | 2.4 |
| B | 5 | 1 | 0.2 | 0.9 | 2.5 |
| C | 10 | 1 | — | 1.8 | 2.5 |
| D | 5 | 0.5 | 0.05 | 1.2 | 1.8 |
| E | 5 | 0.2 | 0.06 | 1.3 | 1.0 |
| F | 5 | 0.1 | 0.1 | 1.3 | 0.7 |

TABLE 2
RESULTS OF FINITE ELEMENT ANALYSIS OF EMBANKMENT WITH
RIGIDLY SUPPORTED CUTOFF WALL

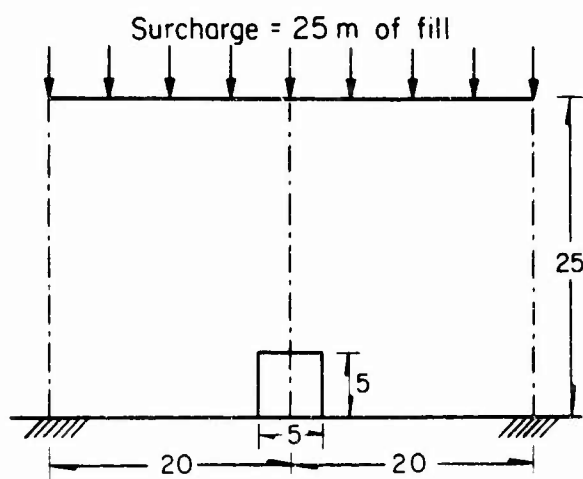
| Case | Tension zone in embankment | | | Tension zone in foundation | | | σ_v | s_{max} | τ_{max} | F | Maximum settlement | |
|------|----------------------------|-------|------------------------|----------------------------|-------|------------------------|------------|-----------|--------------|-------|--------------------|--------------------|
| | width | depth | maximum tensile stress | width | depth | maximum tensile stress | | | | | crest | foundation surface |
| | m | m | kg/sq cm | m | m | kg/sq cm | kg/sq cm | | | kg/cm | m | m |
| A | 72 | 50 | 2.4 | 13 | 40 | 13 | 44 | 4.3 | 21 | 23760 | 5.72 | 3.83 |
| B | 70 | 52 | 2 | 15 | 19 | 30 | 50 | — | — | — | 6.03 | 3.97 |
| C | 70 | 45 | 1.5 | 13 | 50 | 16 | 8.5 | 5.3 | 28 | 26520 | 6.13 | 3.90 |
| D | 60 | 50 | 1.5 | 13 | 44 | 15 | — | 4.5 | 21 | 25400 | 6.37 | 3.98 |



CASE A-Semi-elliptical conduit, $H/D=5$



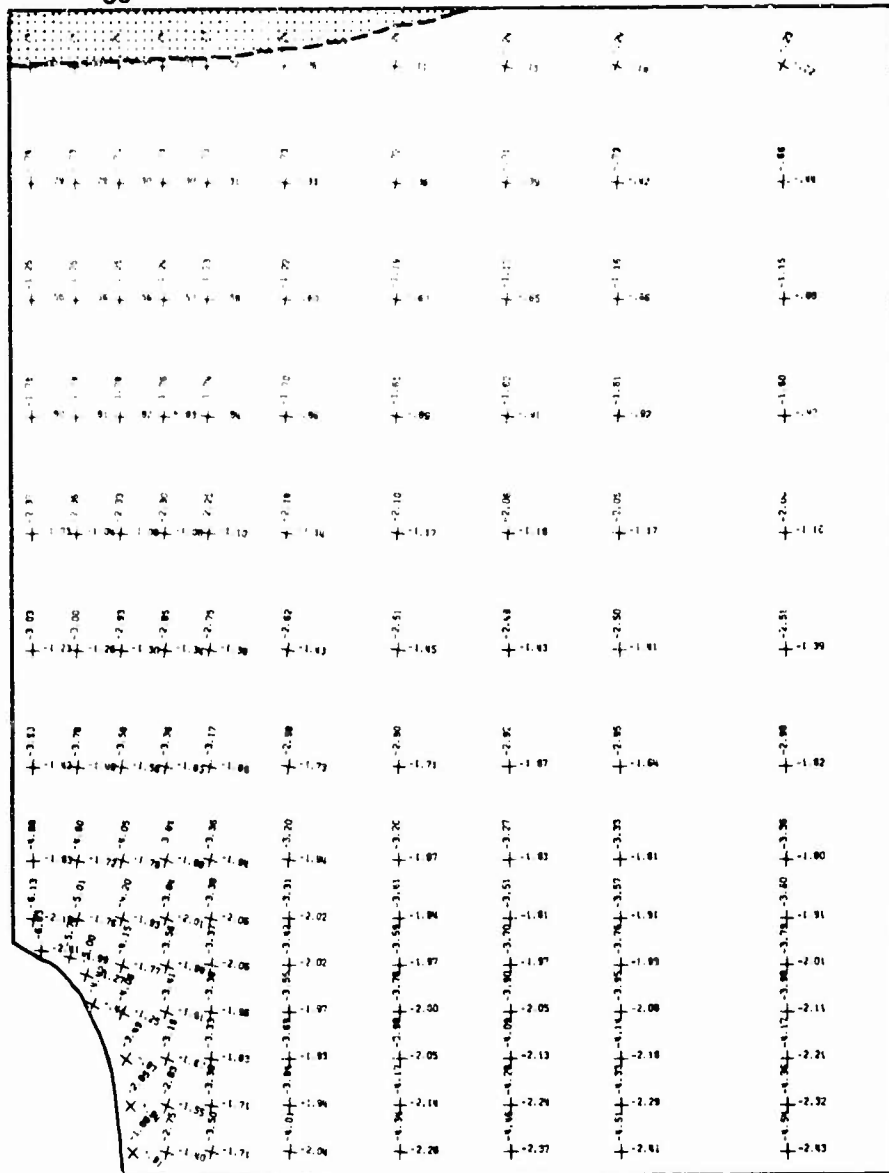
CASE B-Square conduit, $H/D=5$



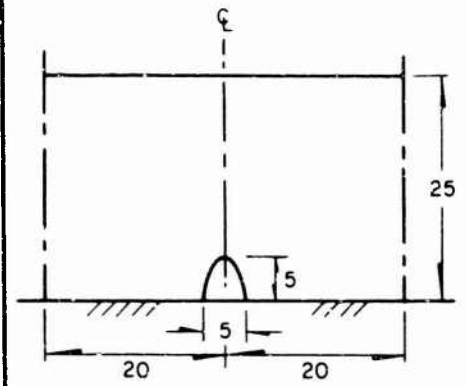
CASE C-Square conduit, $H/D=10$

Dimensions are in meters

Fig. 1 Geometry of conduits studied



LEGEND



Dimensions are in meters

| Young's modulus E kg/sq cm | Poisson's ratio ν | Unit weight γ kg/cu m |
|------------------------------------|--------------------------|------------------------------------|
| 200 | 0.35 | 1900 |

..... Tension zone

-6.72 x 10³
Principal stresses in
kg/sq cm
Tension is positive

Fig. 2(a) Principal stresses in fill surrounding semi-elliptical conduit

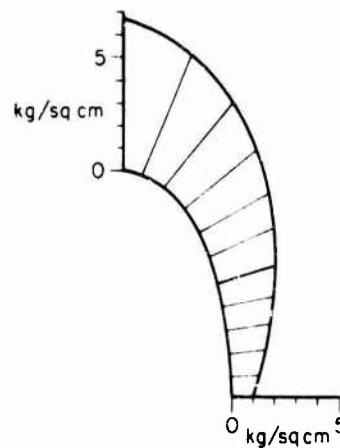
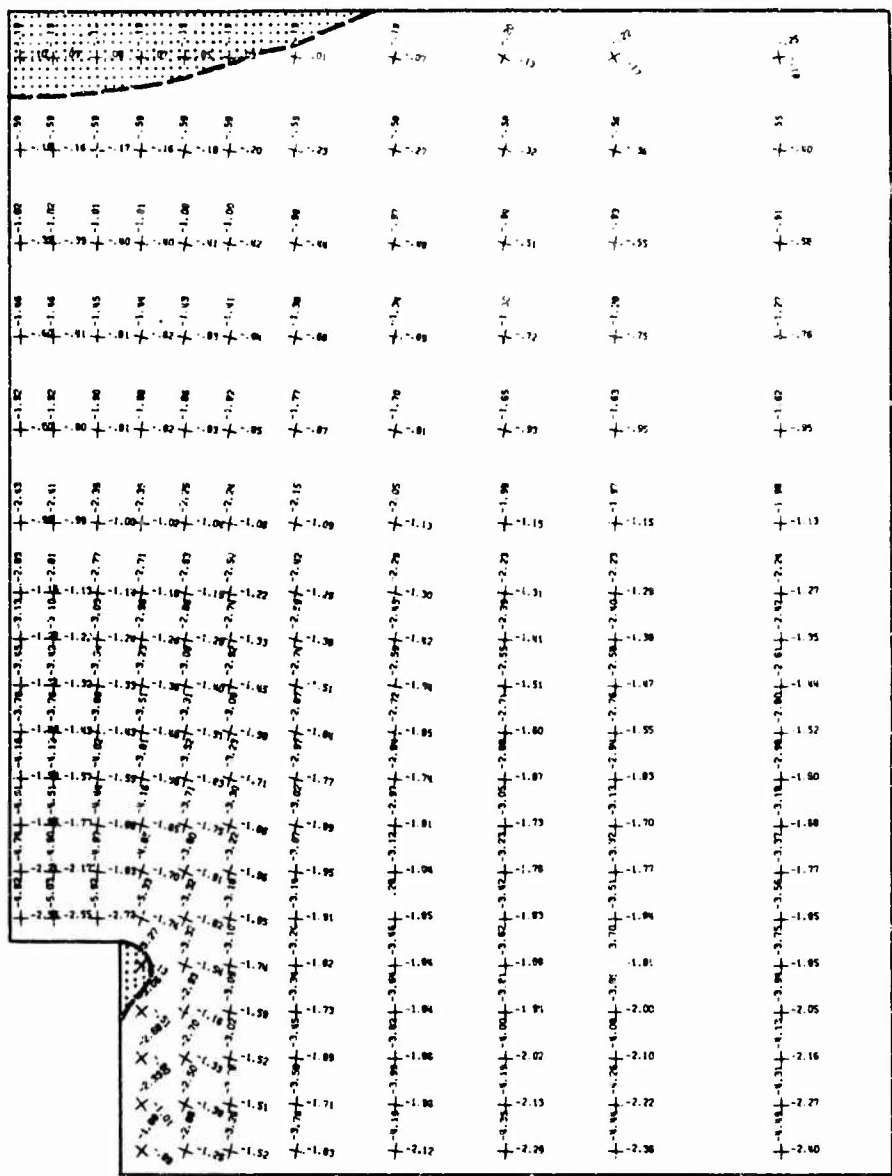
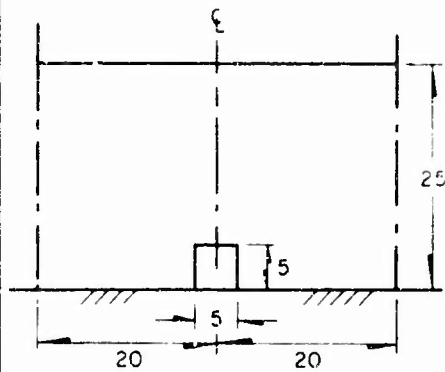


Fig. 2(b) Normal stresses acting on the sides of semi-elliptical conduit



LEGEND



Dimensions are in meters

| Young's modulus E kg/sq cm | Poisson's ratio ν | Unit weight γ kg/cum |
|----------------------------------|--------------------------|-----------------------------------|
| 20C | 0.35 | 1900 |

..... Tension zone
Principal stresses in kg/sq cm
Tension is positive

Fig. 3(a) Principal stresses in fill surrounding square conduit with H/D ratio of 5

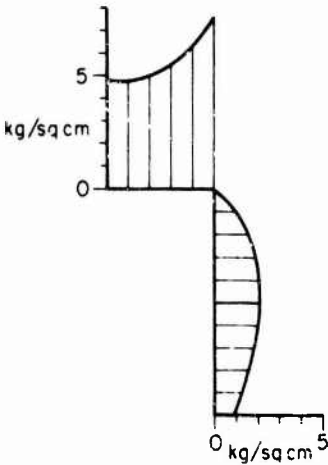
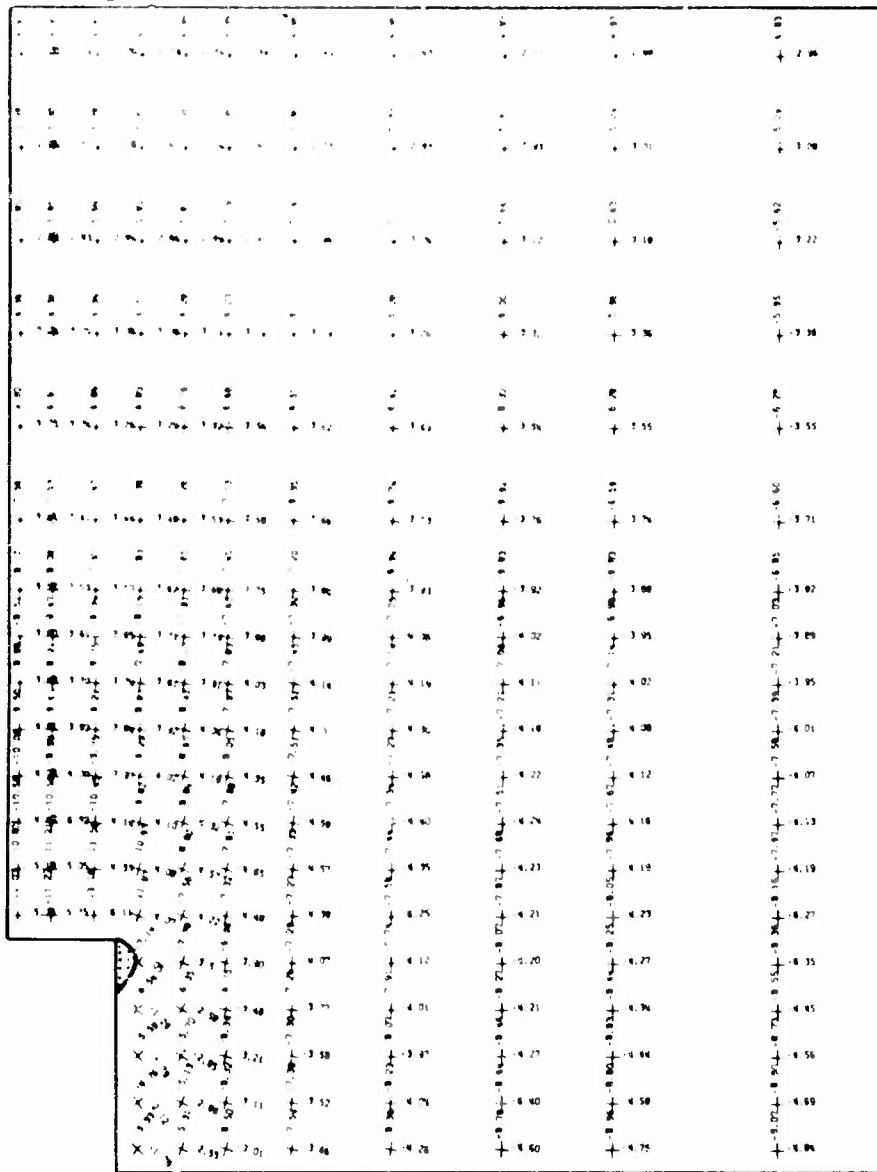
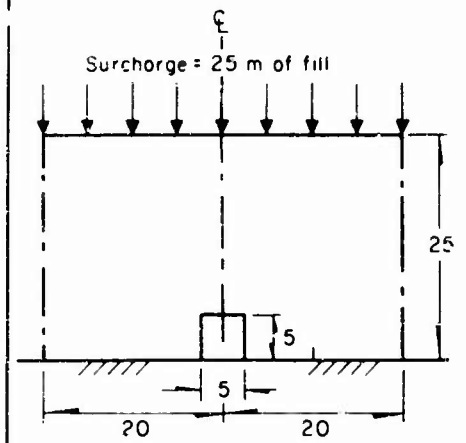


Fig. 3(b) Normal stresses acting on the sides of square conduit with H/D ratio of 5



LEGEND



Dimensions are in meters

| Young's modulus E kg/sq cm | Poisson's ratio ν | Unit weight γ kg/cu m |
|------------------------------------|--------------------------|------------------------------------|
| 200 | 0.35 | 1900 |

..... Tension zone

Principal stresses in kg/sq cm
Tension is positive

Fig. 4(a) Principal stresses in fill surrounding square conduit with H/D ratio of 10

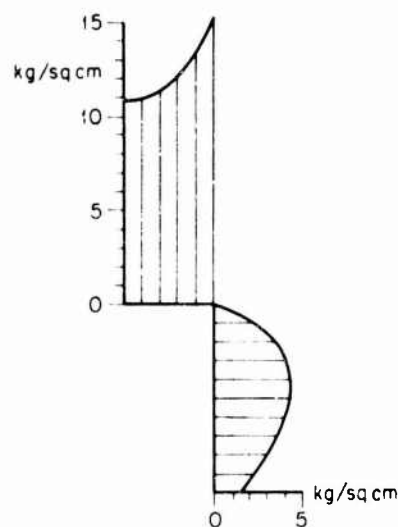
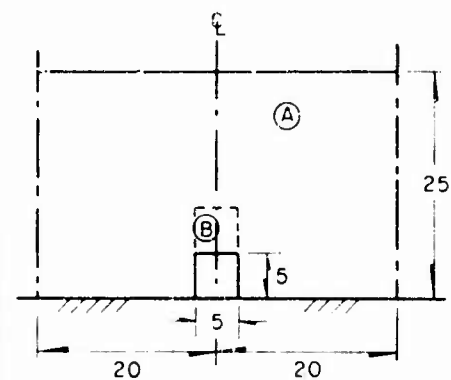


Fig. 4(b) Normal stresses acting on the sides of square conduit with H/D ratio of 10

LEGEND



Dimensions are in meters

| Material in zone | Young's modulus E kg/sqcm | Poisson's ratio ν | Unit weight γ kg/cm |
|------------------|---------------------------|-----------------------|----------------------------|
| (A) | 200 | 0.35 | 1900 |
| (B) | 100 | 0.35 | 1900 |

..... Tension zone

-6.12 +1.53
Principal stresses in kg/sq cm
Tension is positive

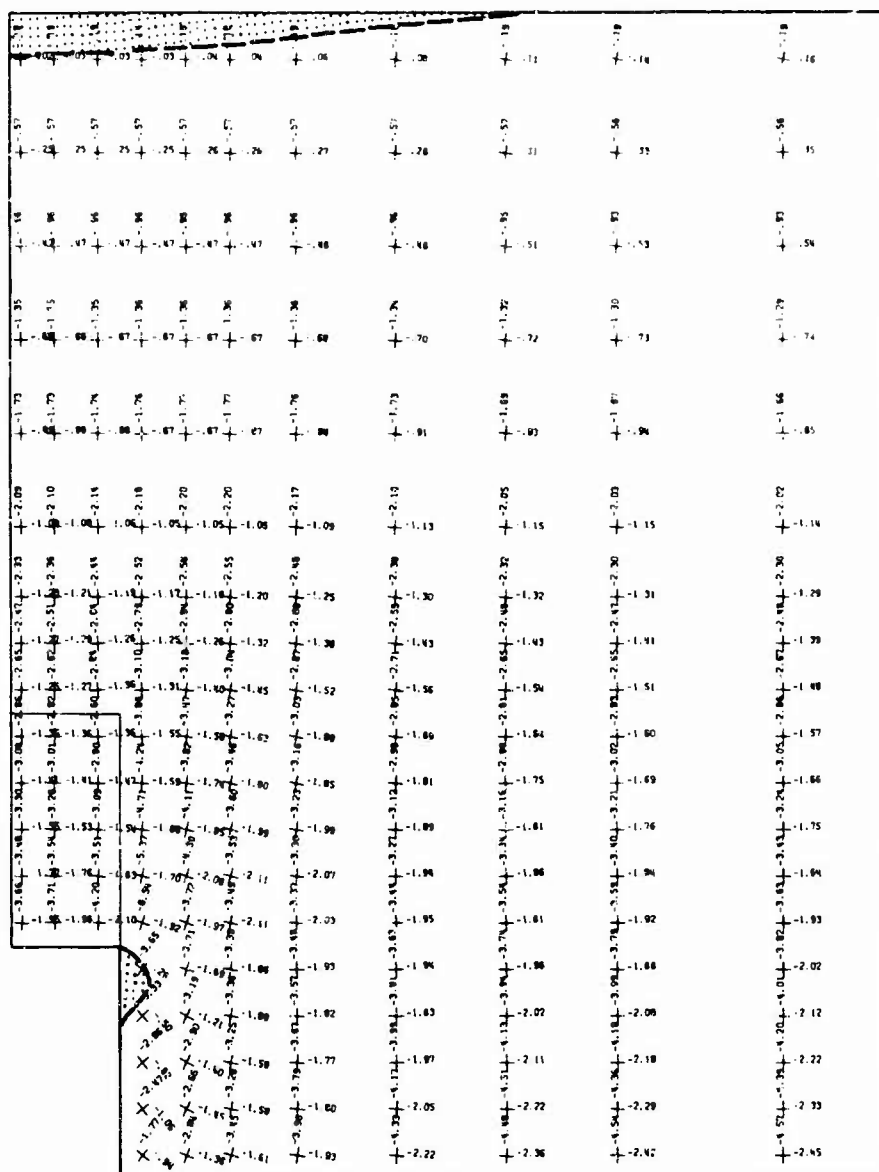


Fig. 5(a) Principal stresses in fill surrounding square conduit; Compressibility ratio of 1/2

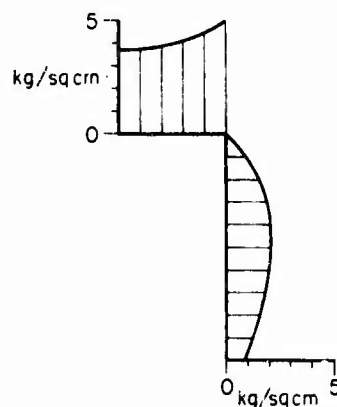
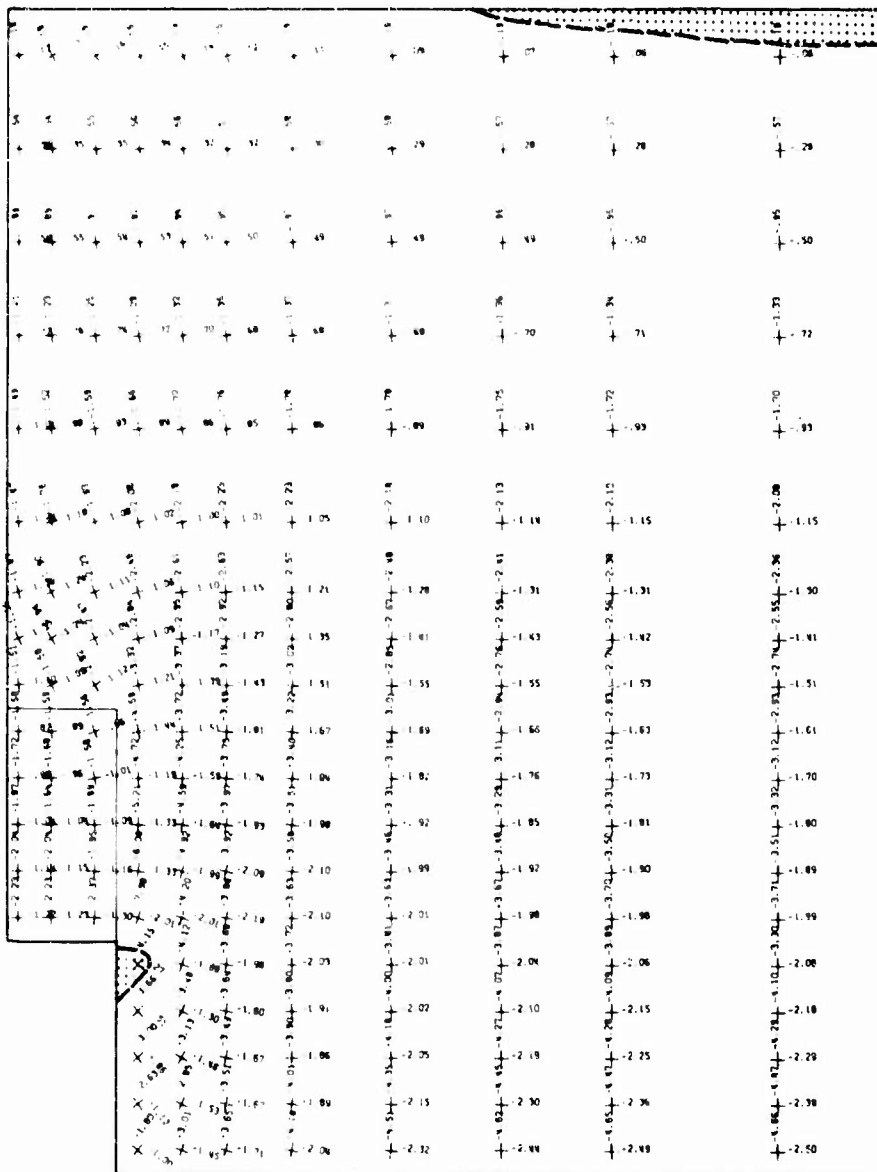
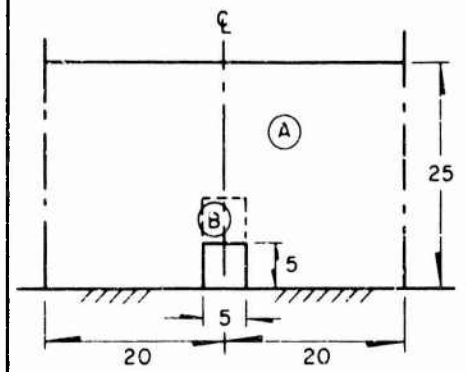


Fig. 5(b) Normal stresses acting on the sides of square conduit; Compressibility ratio of 1/2



LEGEND



Dimensions are in meters

| Material in zone | Young's modulus E kg/sq cm | Poisson's ratio ν | Unit weight γ kg/cu m |
|------------------|----------------------------|-----------------------|------------------------------|
| (A) | 200 | 0.35 | 1900 |
| (B) | 40 | 0.35 | 1900 |

..... Tension zone

-6.72 x 1.53
Principal stresses in kg/sq cm
Tension is positive

Fig. 6(a) Principal stresses in fill surrounding square conduit; Compressibility ratio of 1/5

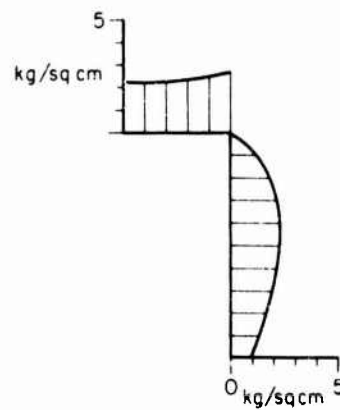
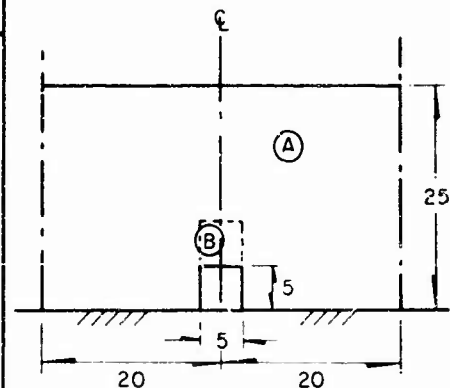
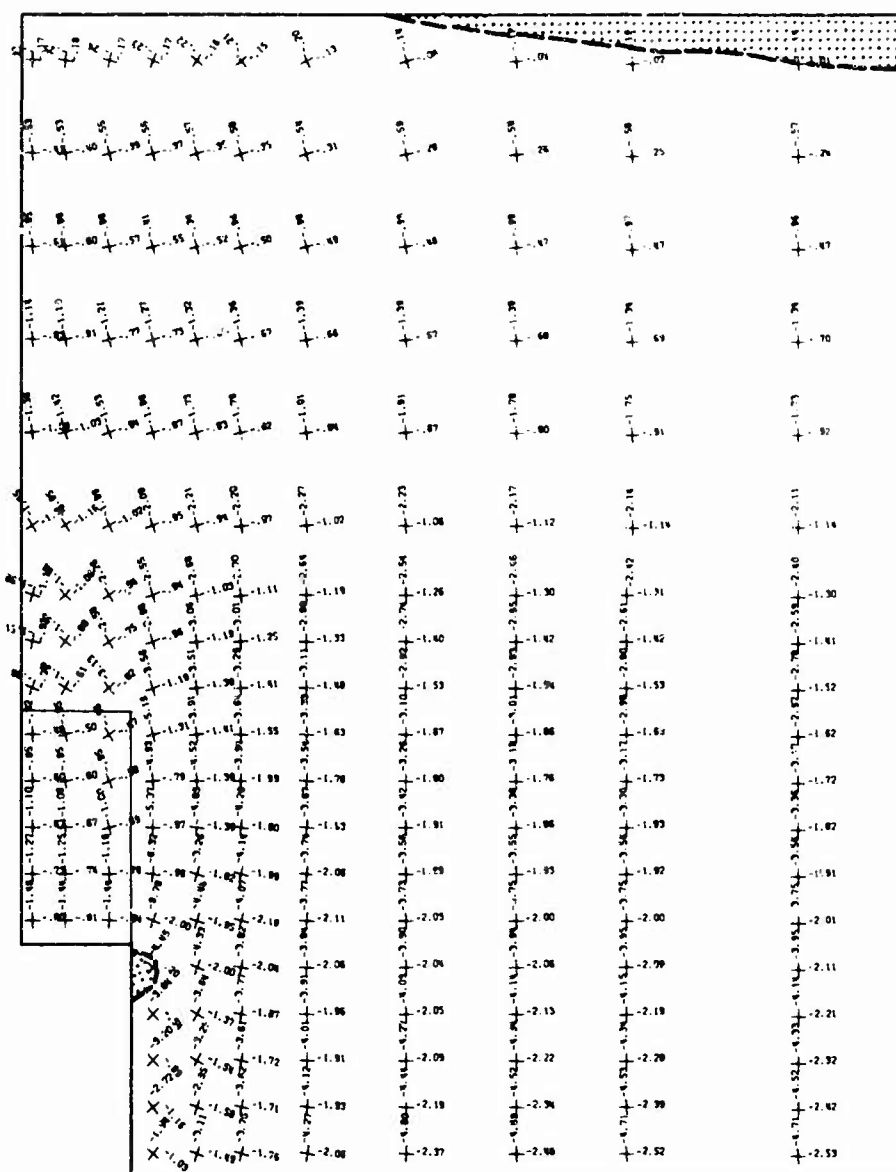


Fig. 6(b) Normal stresses acting on the sides of square conduit; Compressibility ratio of 1/5



Dimensions are in meters

| Material in zone | Young's modulus E kg/sq cm | Poisson's ratio ν | Unit weight γ kg/cum |
|------------------|----------------------------|-----------------------|-----------------------------|
| (A) | 200 | 0.35 | 1900 |
| (B) | 20 | 0.35 | 1900 |

..... Tension zone

-6.72 x 1.53
Principal stresses in kg/sq cm
Tension is positive

Fig. 7(a) Principal stresses in fill surrounding square conduit; Compressibility ratio of 1/10

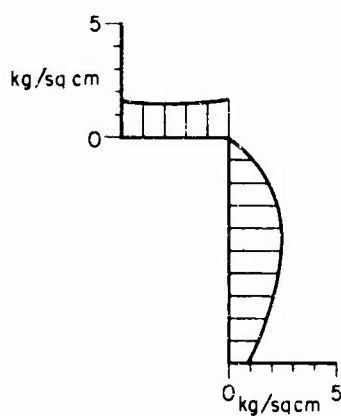


Fig. 7(b) Normal stresses acting on the sides of square conduit; Compressibility ratio of 1/10

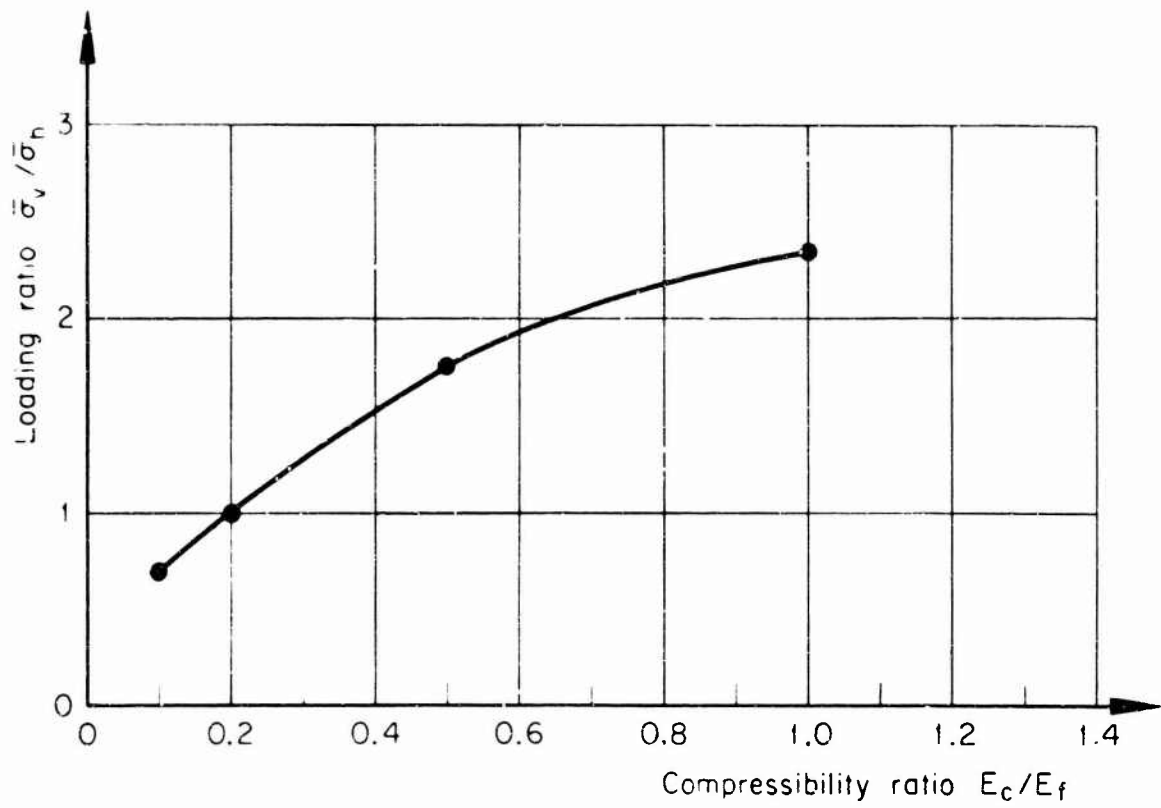


Fig.8 Loading ratio for square conduit as function of compressibility ratio

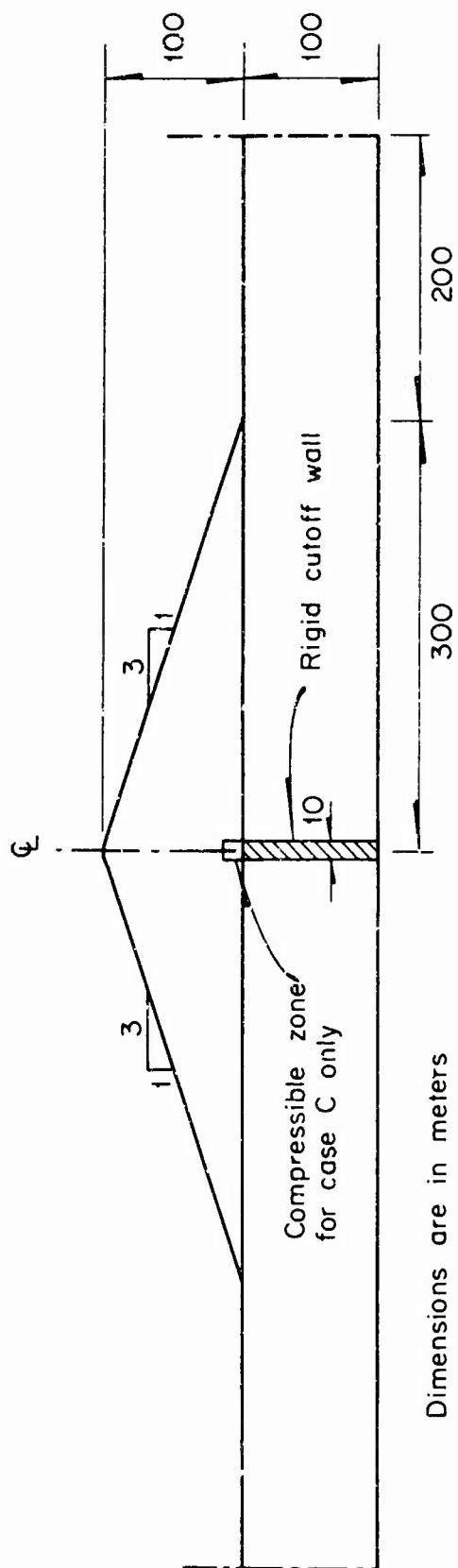


Fig.9(a) Geometry of dam used in Cases A, B and C

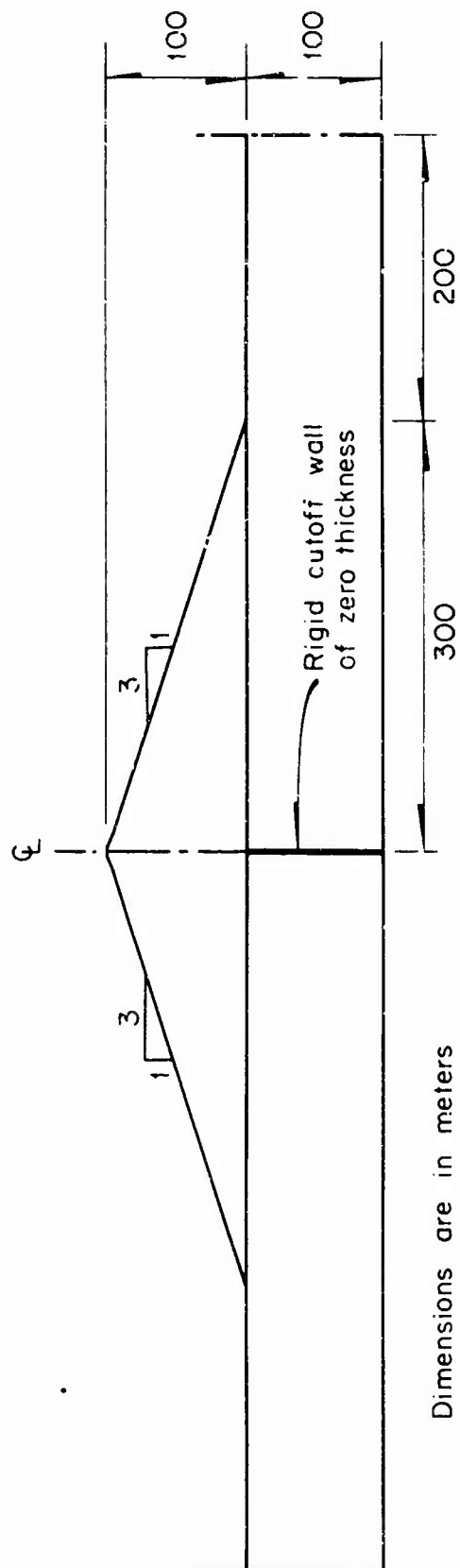


Fig.9(b) Geometry of dam used in Case D

Fig. 10(a) Displacements in dam and foundation, Case A

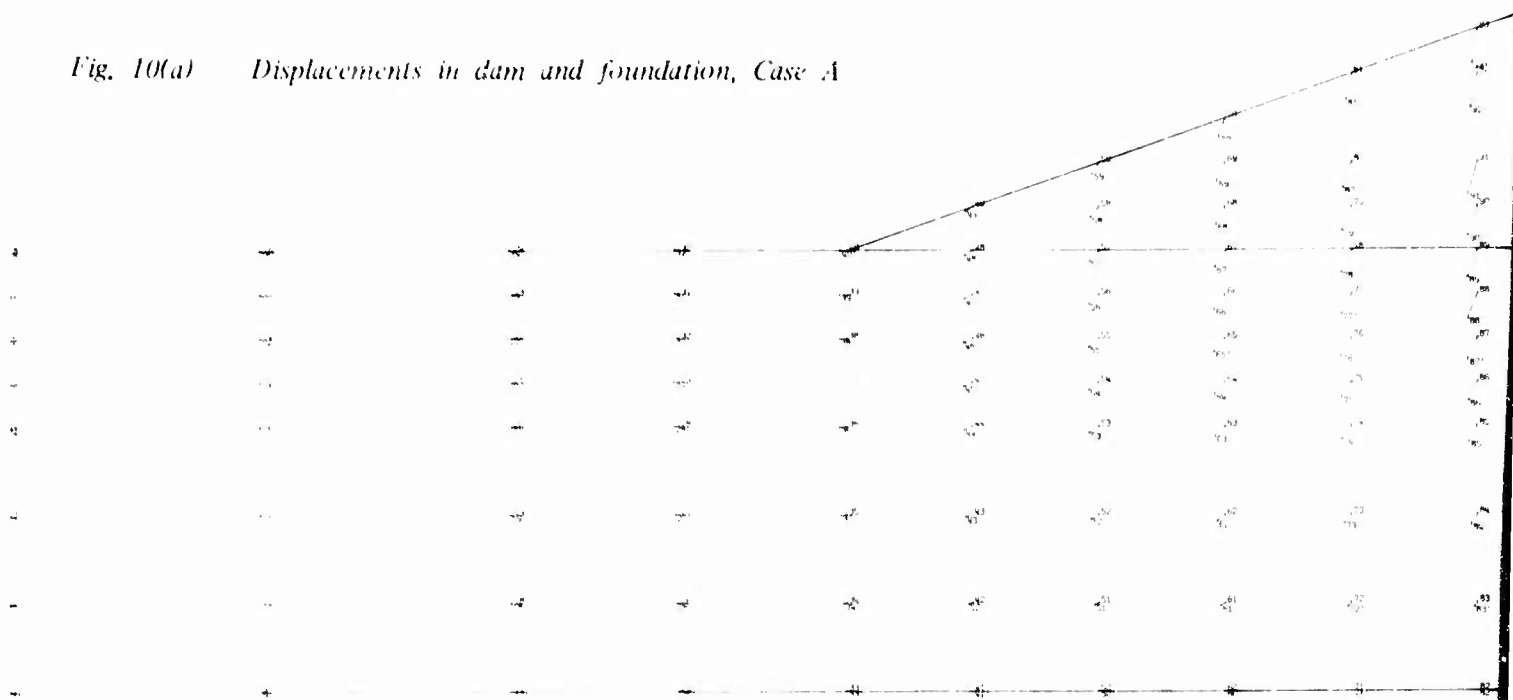
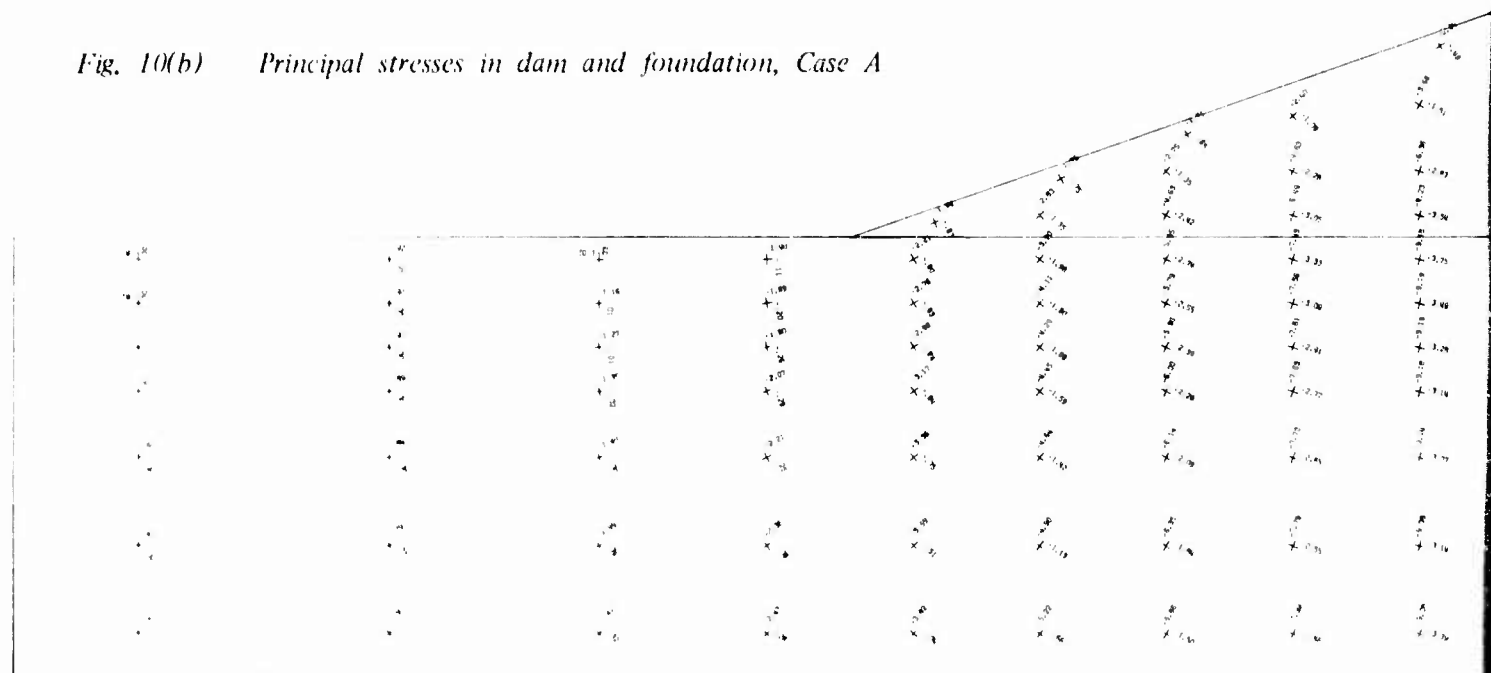
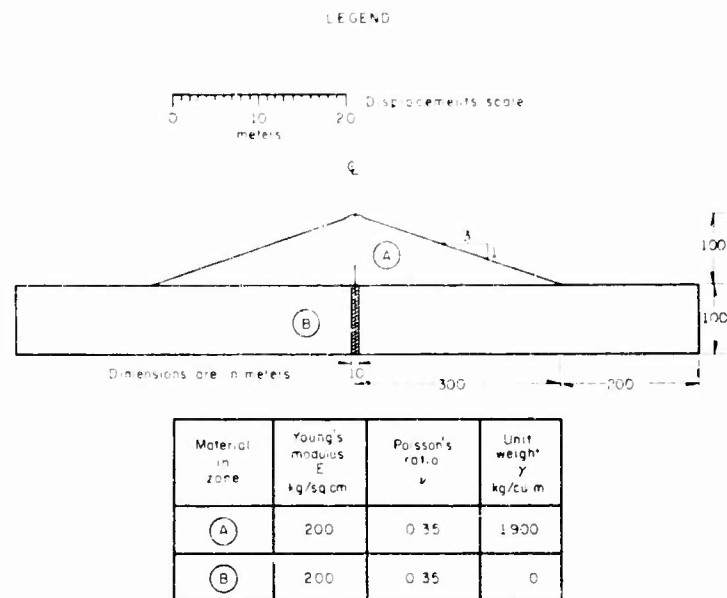
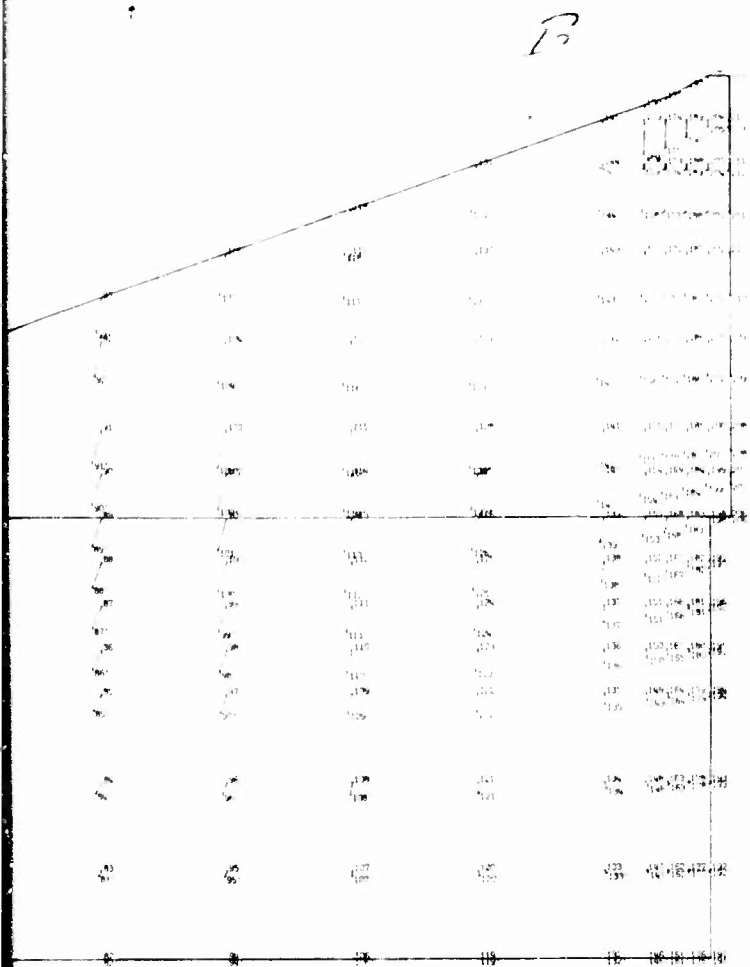


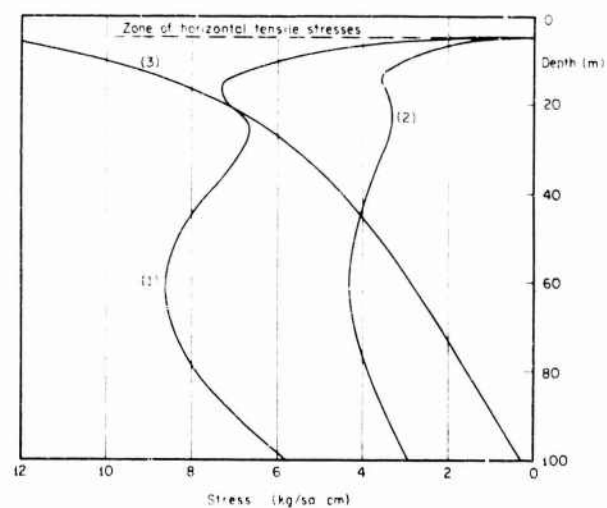
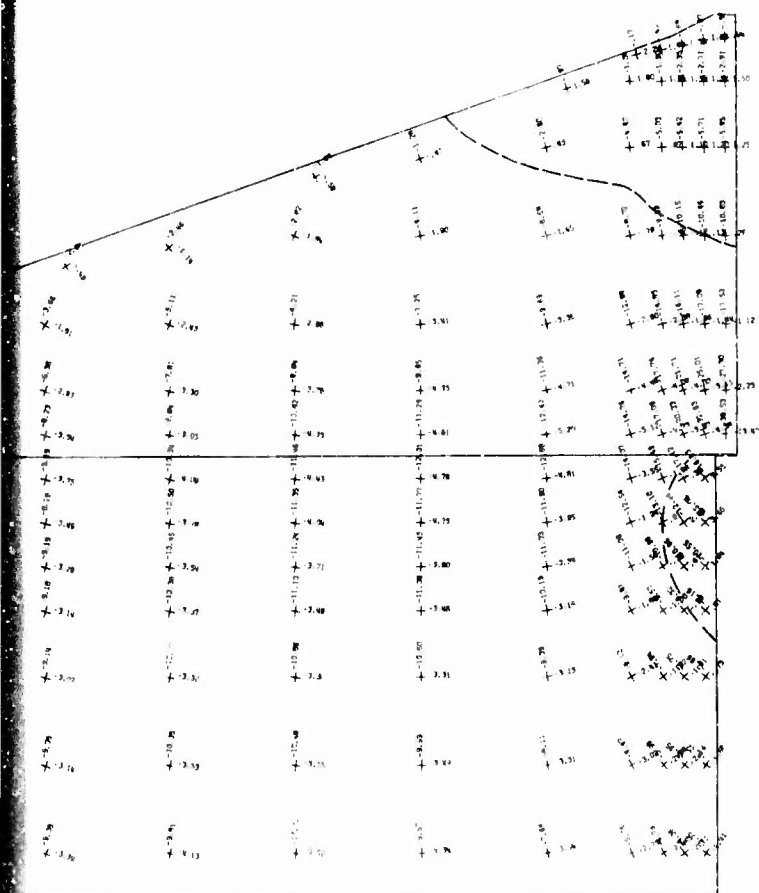
Fig. 10(b) Principal stresses in dam and foundation, Case A





Tension zone

Principal stresses in kg/sq cm
Tension is positive



- (1) Effective horizontal stress acting on wall
- (2) Potential maximum shearing resistance
- (3) Shear stress produced by weight of embankment

Fig. 10(c) Stresses acting on one side of the wall, Case A

Fig. 11(a) Displacements in dam and foundation, Case B

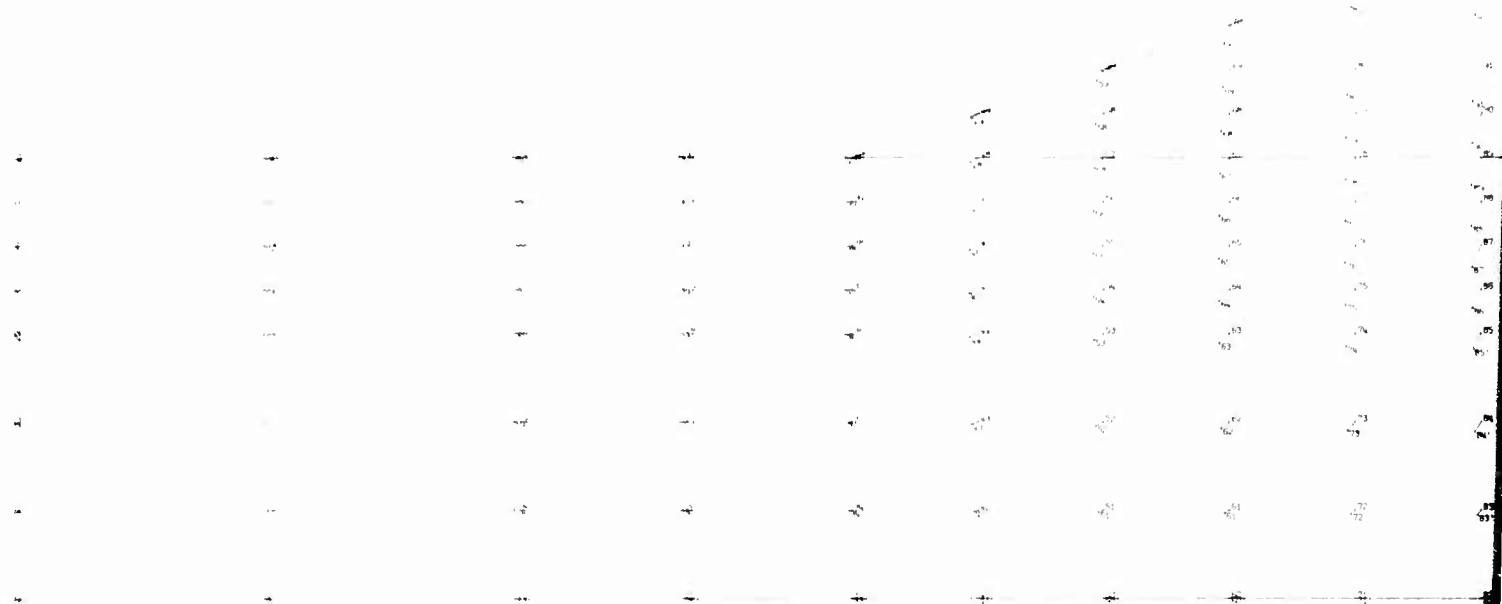
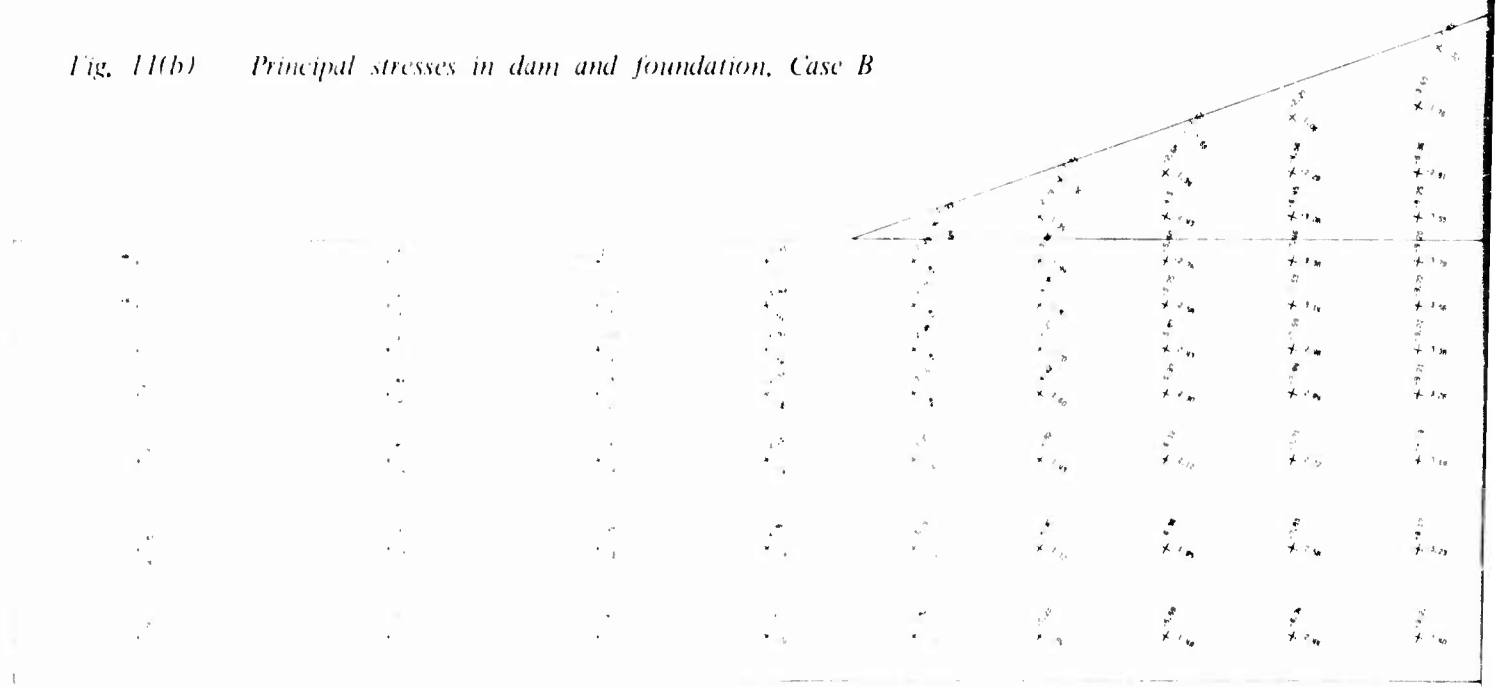
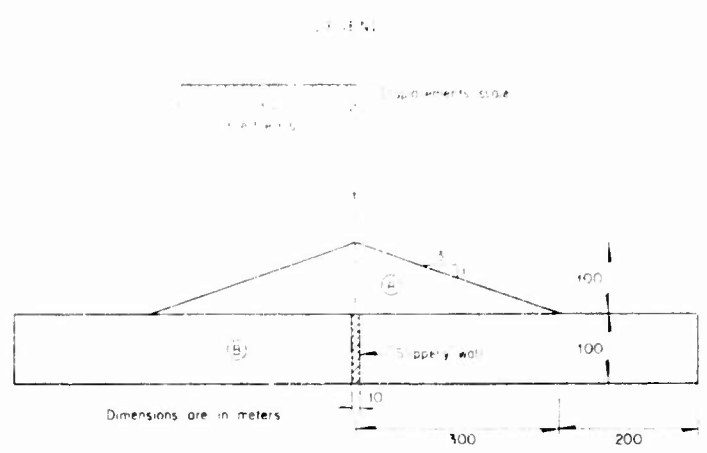
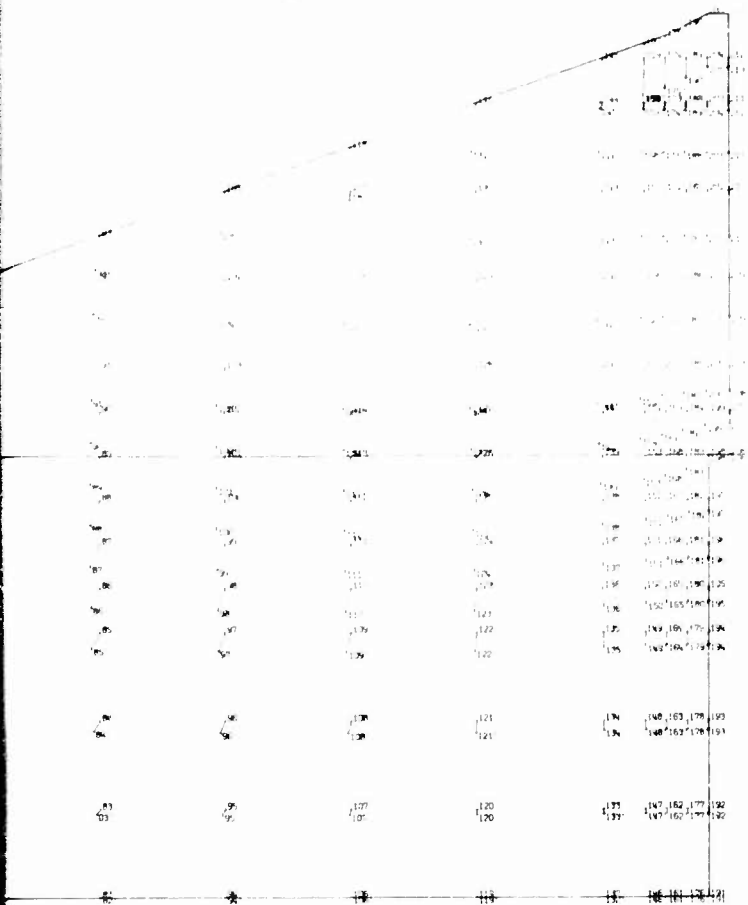


Fig. 11(b) Principal stresses in dam and foundation, Case B



13



| Material in zone | Young's modulus E kg/sq cm | Poisson's ratio ν | Unit weight γ kg/cu m |
|------------------|----------------------------|-----------------------|------------------------------|
| (A) | 200 | 0.35 | 1900 |
| (B) | 200 | 0.35 | 0 |

Tension zone
Principal stresses in kg/sq cm
Tension is positive

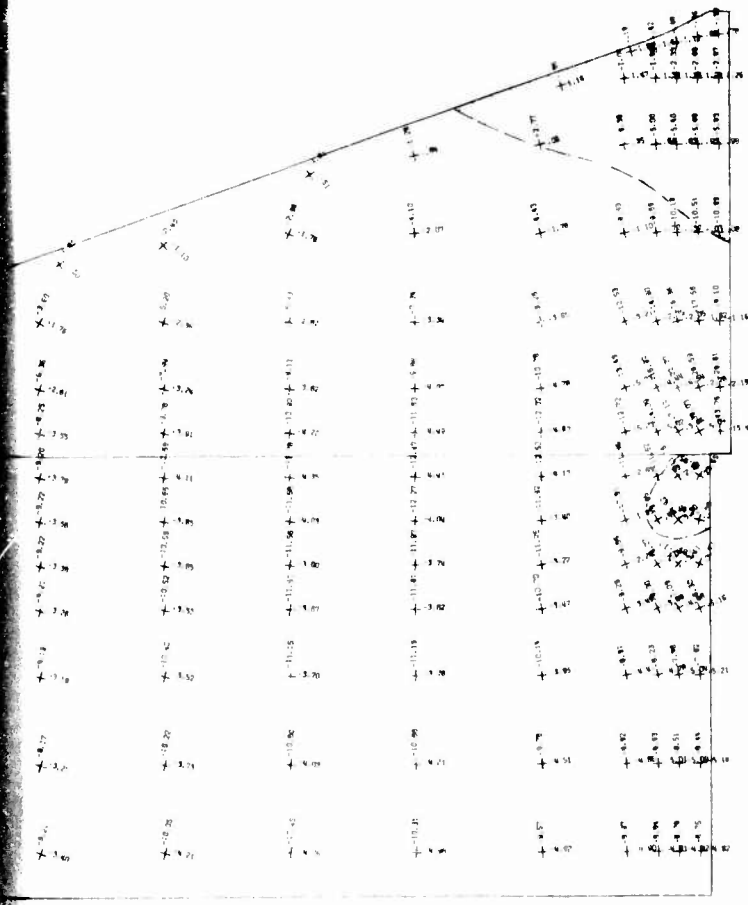


Fig. 12(a) Displacements in dam and foundation, Case C

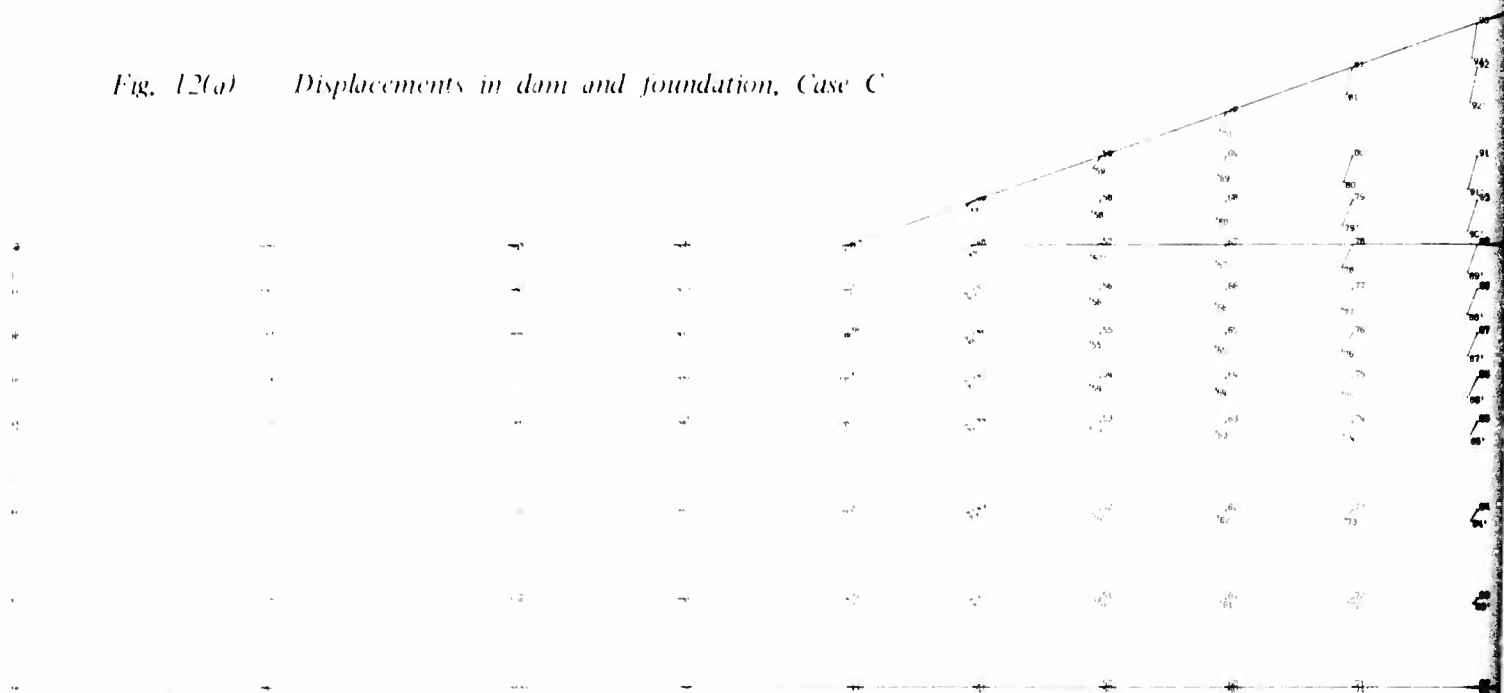
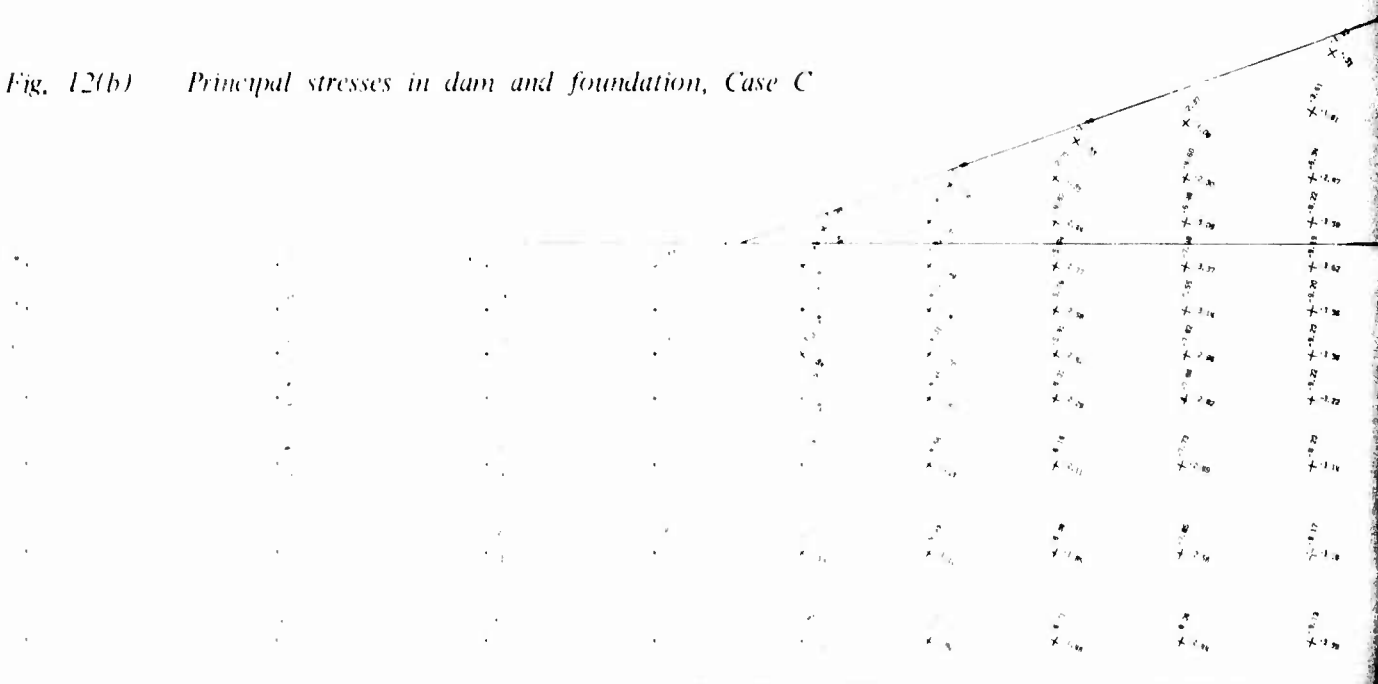
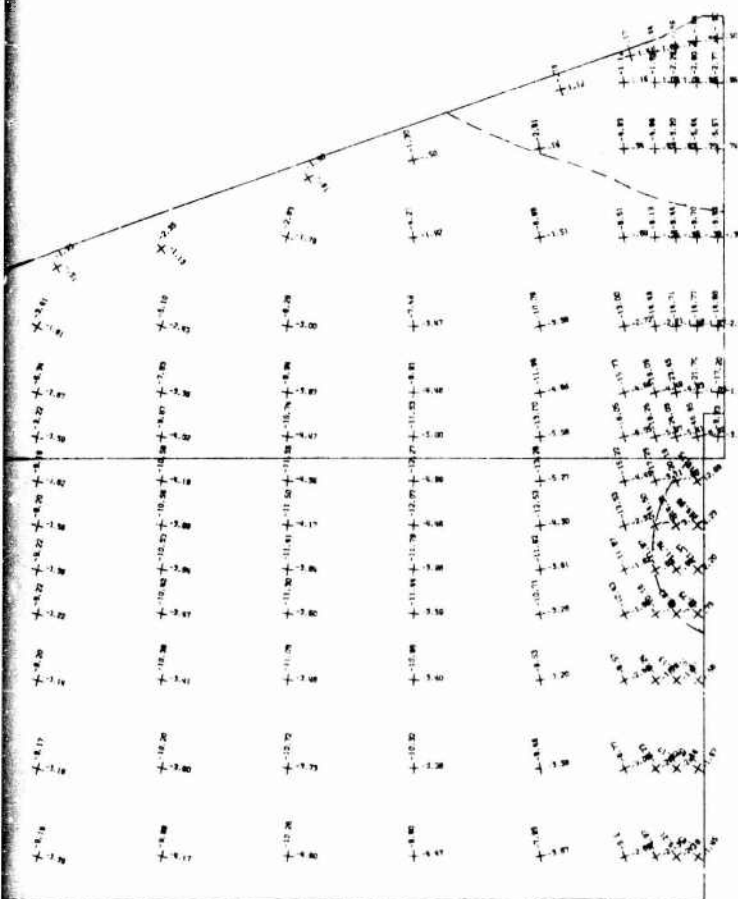
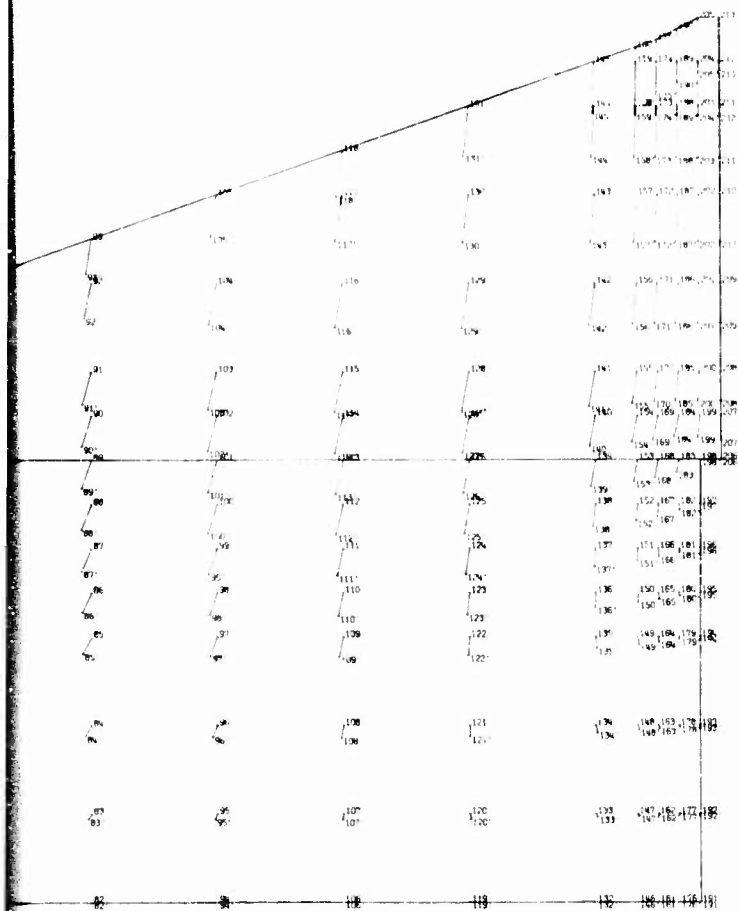
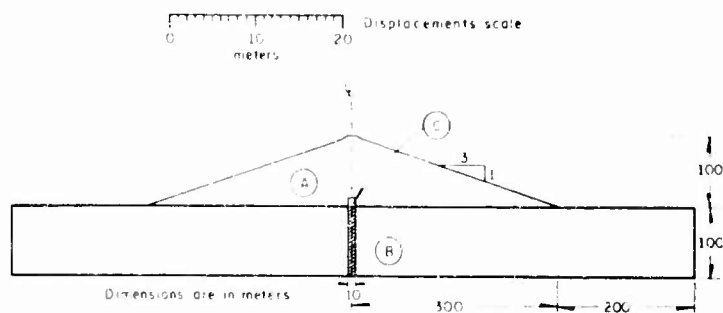


Fig. 12(b) Principal stresses in dam and foundation, Case C





LEGEND

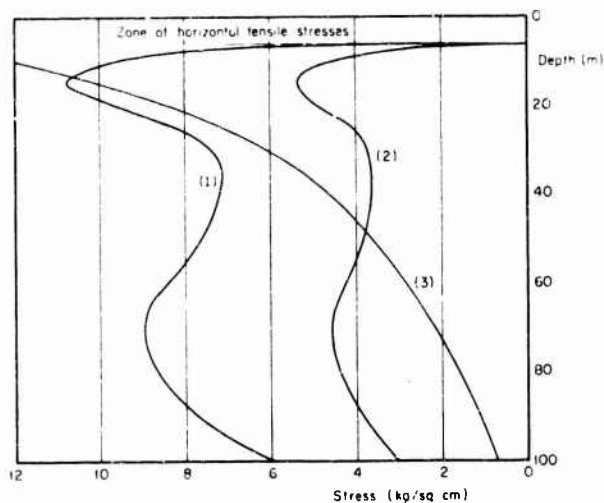


| Material in zone | Young's modulus E kg/sq cm | Poisson's ratio ν | Unit weight γ kg/cu m |
|------------------|----------------------------|-----------------------|------------------------------|
| (A) | 200 | 0.35 | 1900 |
| (B) | 200 | 0.35 | 0 |
| (C) | 20 | 0.35 | 1900 |

Tension zone



Principal stresses in kg/sq cm
Tension is positive



- (1) Effective horizontal stress acting on wall
- (2) Potential maximum shearing resistance
- (3) Shear stress produced by weight of embankment

Fig. 12(c) Stresses acting on one side of the wall, Case C

Fig. 13(a) Displacements in dam and foundation, Case D

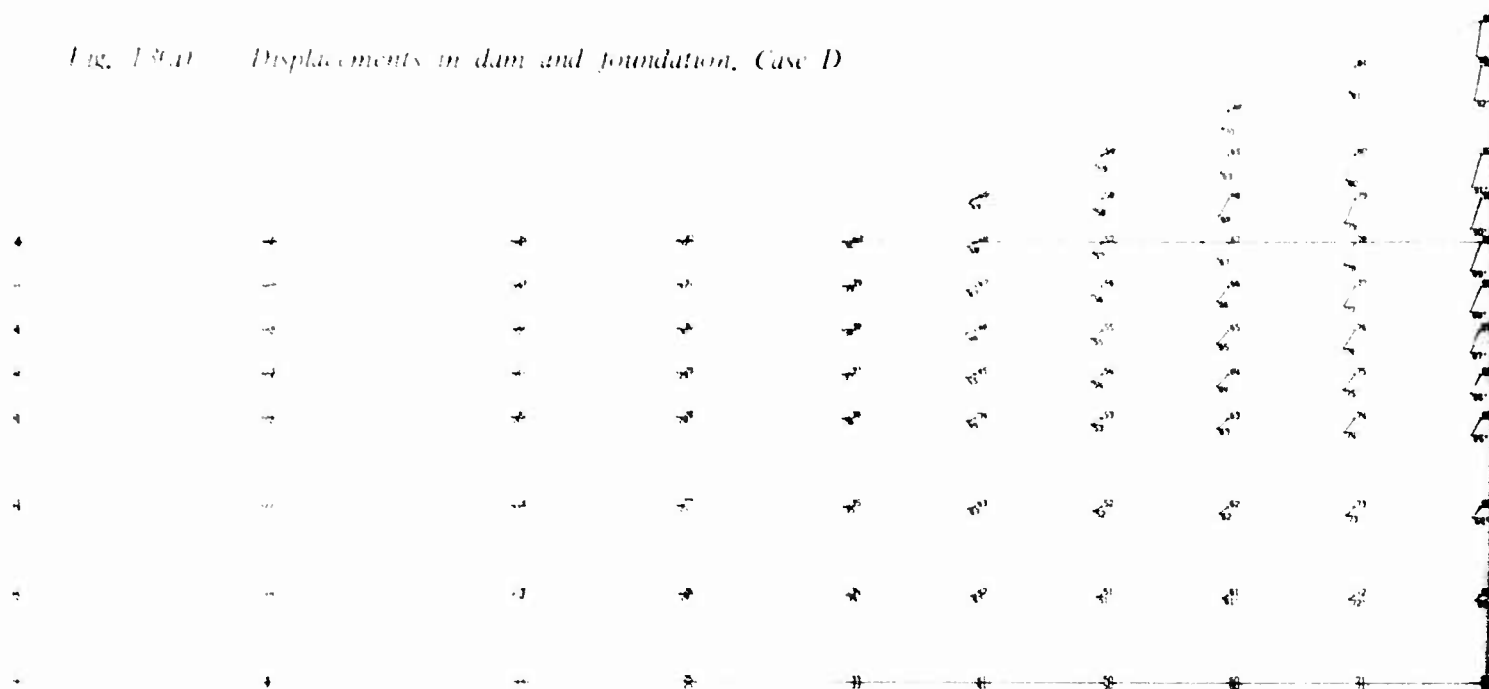
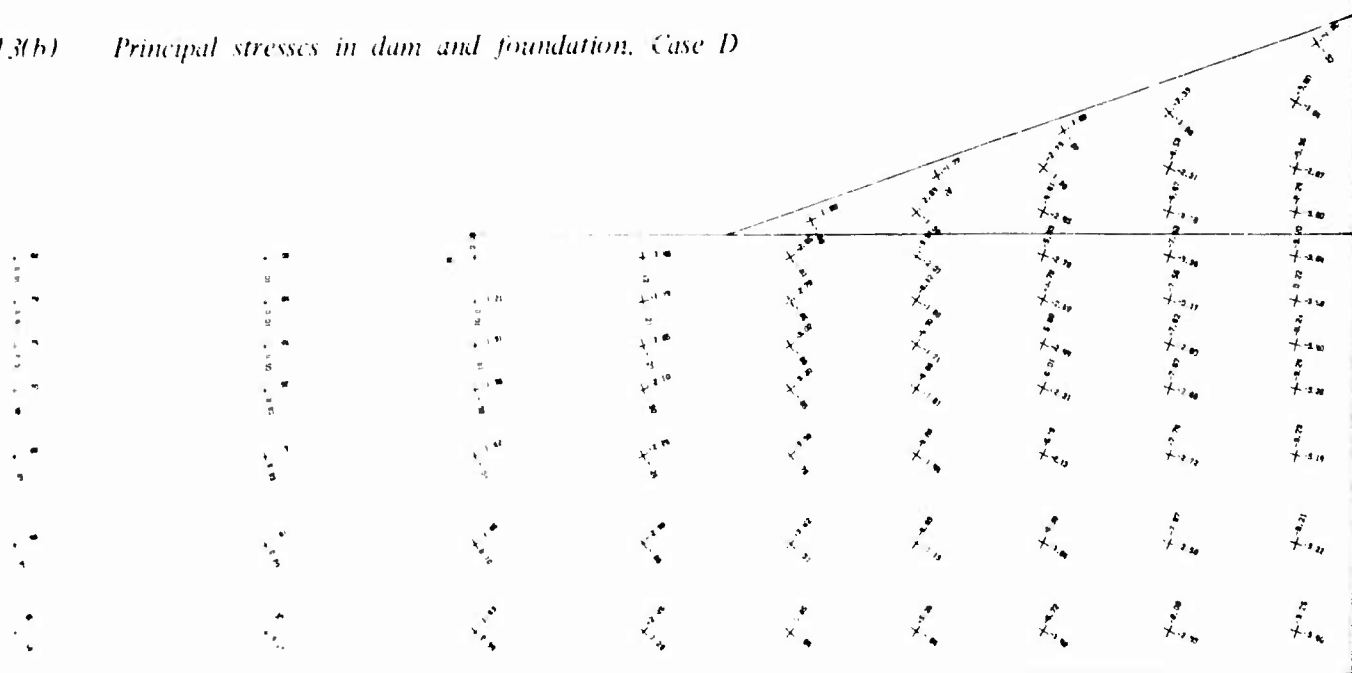
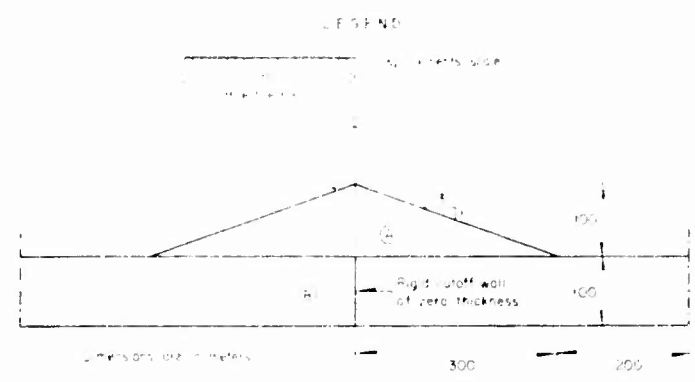
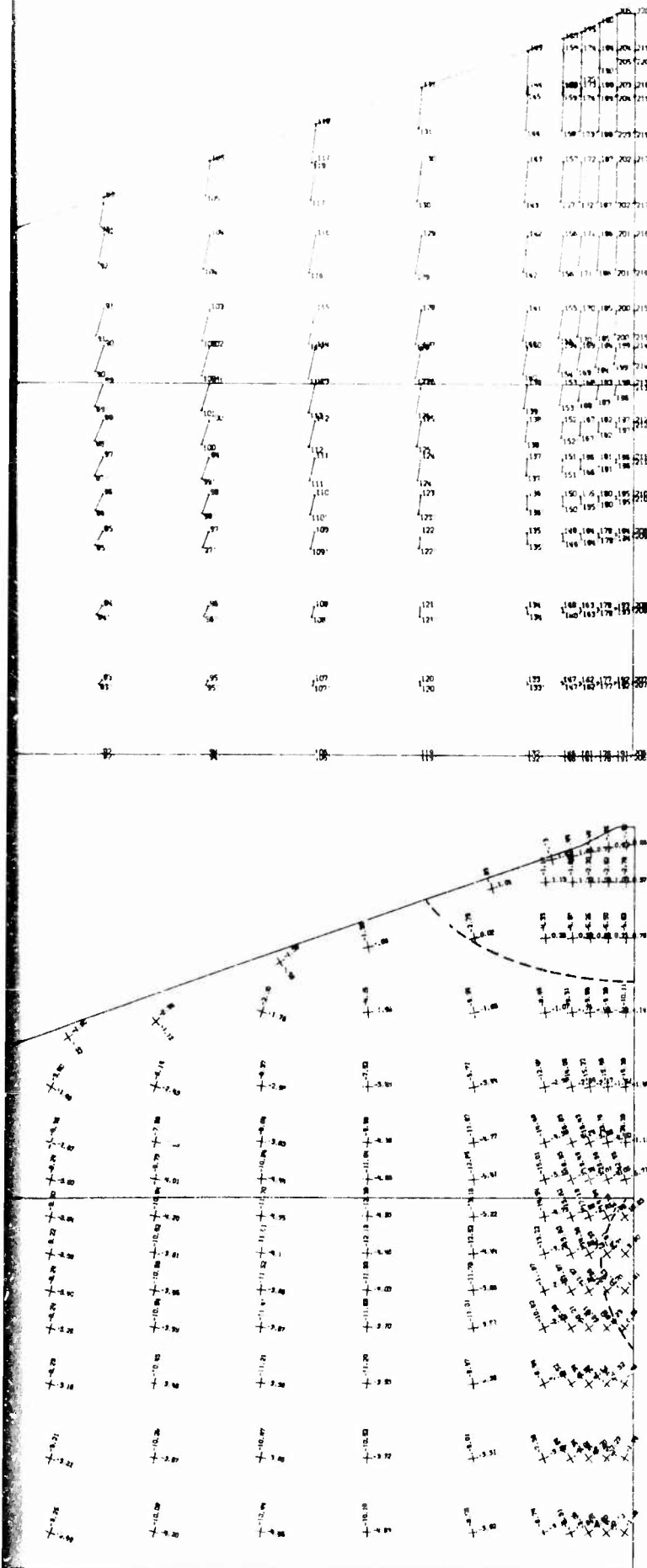


Fig. 13(b) Principal stresses in dam and foundation, Case D

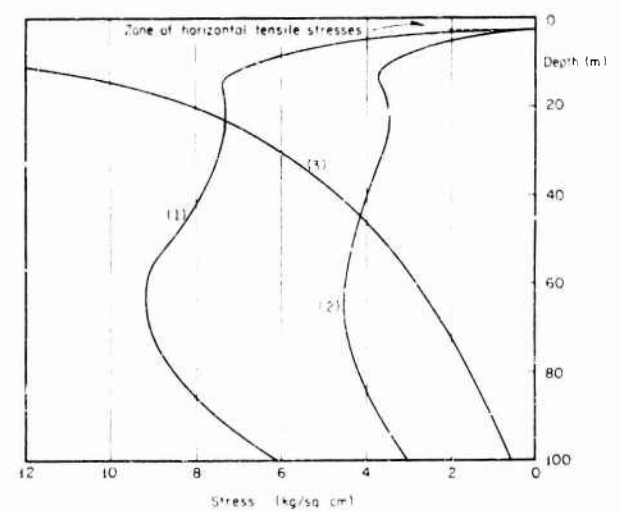


β



| Material in zone | Young's modulus E kg/sq cm | Poisson's ratio ν | Unit weight γ kg/cm ³ |
|------------------|----------------------------|-----------------------|---|
| (A) | 200 | 0.35 | 1900 |
| (B) | 200 | 0.35 | 0 |

Tension zone
Principal stresses in kg/sq cm
Tension positive



- (1) Effective horizontal stress acting on wall
- (2) Potential maximum shearing resistance
- (3) Shear stress produced by weight of embankment

Fig. 13(c) Stresses acting on one side of the wall, Case D

Unclassified

Security Classification

| DOCUMENT CONTROL DATA - R & D | | |
|--|------------------------|---|
| <i>(Security classification of title, body of abstract and indexing annotation must be entered when the overall report is classified)</i> | | |
| 1. ORIGINATING ACTIVITY (Corporate author) | | 2a. REPORT SECURITY CLASSIFICATION |
| Harvard University Cambridge, Massachusetts | | Unclassified |
| | | 2b. GROUP |
| 3. REPORT TITLE | | |
| CRACKING OF FAHNE AND ROCKHILL DAMS; TENSION ZONES IN EMBANKMENTS CAUSED BY CONDUITS AND CUTOFF WALLS | | |
| 4. DESCRIPTIVE NOTES (Type of report and inclusive dates) | | |
| Final report | | |
| 5. AUTHOR(S) (First name, middle initial, last name) | | |
| Arthur Casagrande Sergio M. Covarrubias | | |
| 6. REPORT DATE | 7a. TOTAL NO. OF PAGES | 7b. NO. OF REFS |
| July 1970 | 29 | 0 |
| 8a. CONTRACT OR GRANT NO. | | 9a. ORIGINATOR'S REPORT NUMBER(S) |
| DACW 29-69-C-0029 | | |
| b. PROJECT NO. | | 9b. OTHER REPORT NO(S) (Any other numbers that may be assigned this report) |
| c. Item No. EC-644 | | |
| d. | | |
| 10. DISTRIBUTION STATEMENT | | |
| This document has been approved for public release and sale; its distribution is unlimited. | | |
| 11. SUPPLEMENTARY NOTES | | 12. SPONSORING MILITARY ACTIVITY |
| Prepared under contract for U. S. Army Engineer Waterways Experiment Station, Vicksburg, Mississippi | | Office, Chief of Engineers, U. S. Army Washington, D. C. |
| 13. ABSTRACT | | |
| <p>The purpose of this study was to investigate by means of the finite element method (1) the effect of rigid conduits and cutoff walls on the stress distribution and on the development of tension zones in embankments, and their foundations, and (2) the distribution of stresses acting on the sides of conduits and cutoff walls. All materials were assumed to be linearly elastic with equal properties in tension and in compression. The only load considered was the weight of the embankment and it was assumed to be applied in a single lift. Detailed investigation by means of the finite element method included six cases of conduits and four cases of cutoff walls. In the case of conduits, it was demonstrated that tension zones occur adjacent to conduits with sharp edges, and that the presence of a zone of more compressible material above the roof effectively improves the loading conditions on the conduit. In the case of cutoff walls beneath embankments, it was shown that tension zones develop in the upper part of the embankment and adjacent to the top of the wall. While the presence of a zone of more compressible material on top of the wall reduces the load on the upper surface of the wall, it somewhat increases the friction forces along the sides of the wall.</p> | | |

DD FORM 1473

REPLACES DD FORM 1473, 1 JAN 64, WHICH IS OBSOLETE FOR ARMY USE.

Unclassified
Security Classification

Unclassified
Security Classification

| 14. | KEY WORDS | LINK A | | LINK B | | LINK C | |
|-----|-----------------------|--------|----|--------|----|--------|----|
| | | ROLE | WT | ROLE | WT | ROLE | WT |
| | Conduits | | | | | | |
| | Cracks | | | | | | |
| | Cutoff walls | | | | | | |
| | Earth dams | | | | | | |
| | Embankment cracking | | | | | | |
| | Finite element method | | | | | | |
| | Rockfill dams | | | | | | |
| | Stress distribution | | | | | | |

Unclassified
Security Classification